

MASTER

Parameterization of short-range time-irreversibility in nuclear forces\*

Judith Binstock

Los Alamos Scientific Laboratory, Los Alamos, New Mexico 87544, U.S.A.

Ronald Bryan\*

Department of Physics, Texas A&M University,

College Station, Texas 77843, U.S.A.

and

Alexander Gersten<sup>§</sup>

Department of Physics, Ben-Gurion University of the Negev,

Beer-Sheva, Israel

NOTICE  
 This report was prepared as an account of work sponsored by the United States Government. Neither the United States nor the United States Energy Research and Development Administration, nor any of their employees, nor any of their contractors, subcontractors, or their employees, makes any warranty, express or implied, or assumes any legal liability or responsibility for the accuracy, completeness or usefulness of any information, apparatus, product or process disclosed, or represents that its use would not infringe privately owned rights.

MASTER

\* Supported in part by the U.S. Energy Research and Development Administration, contract E (40-1) - 5223

<sup>§</sup> On leave at the Laboratoire de Physique Théorique des Particules Élémentaires, Université Pierre et Marie Curie, 4. Place Jussieu, 75230 Paris CEDEX 05, France

CP

6309

## **DISCLAIMER**

**This report was prepared as an account of work sponsored by an agency of the United States Government. Neither the United States Government nor any agency Thereof, nor any of their employees, makes any warranty, express or implied, or assumes any legal liability or responsibility for the accuracy, completeness, or usefulness of any information, apparatus, product, or process disclosed, or represents that its use would not infringe privately owned rights. Reference herein to any specific commercial product, process, or service by trade name, trademark, manufacturer, or otherwise does not necessarily constitute or imply its endorsement, recommendation, or favoring by the United States Government or any agency thereof. The views and opinions of authors expressed herein do not necessarily state or reflect those of the United States Government or any agency thereof.**

## **DISCLAIMER**

**Portions of this document may be illegible in electronic image products. Images are produced from the best available original document.**

Abstract: The observation that, in a time-irreversible one-boson-exchange nucleon-nucleon potential model due to Bryan and Gersten, T-violation occurs mostly in the lowest-permitted angular momentum states, leads us to construct a phase-shift parameterization of the 50 to 450 MeV NN data where T-violation takes place only in the lowest possible angular momentum states. The five ordinary (T-symmetric) Wolfenstein amplitudes are taken from phase shift analysis, and the sixth, T-asymmetric amplitude,  $t(\theta)$ , is parameterized by a single infinitesimal phase parameter  $\lambda_1$  ( $\lambda_2$ ) in the case of np (pp) scattering. This leads to unique predictions for the relative angular distributions of time-reversal-asymmetric observables  $P - \mathcal{A}$  and  $P_A - P_B$ , even though the absolute magnitudes remain undetermined. The model corresponds to an ordinary interaction that yields the usual experimental data, plus a superimposed very short-range T-noninvariant force. As such, it directs experimentalists to those angular regions of pp and np  $P - \mathcal{A}$  and  $P_A - P_B$  measurements where T-violation due to short-range forces will be most strongly manifest. As the model incorporates isospin invariance, known to hold only at the few-percent level in np scattering, the predictions are likely to have the greatest significance in the case of pp scattering.

## 1. Introduction

In 1968 Sudarshan proposed a theory<sup>1)</sup> for strong, weak, and electromagnetic interactions wherein the CP violation observed in neutral kaon

decay was assumed to be a property of weak interactions in general, and in particular due to the exchange of the  $A_1(1070)$  axial-vector meson. The interesting thing about the theory was that the CP-violating  $A_1$ -hadronic interaction was assumed to take place in the strong interaction. Specifically, the interaction Lagrangian was

$$\mathcal{L}^{int} = (4\pi)^{1/2} \bar{\psi} \left[ i g_A \gamma_5 \gamma^\mu \tilde{\psi} \cdot A_\mu + (f_A/4m) \gamma_5 \sigma^{\mu\nu} \tilde{\psi} \cdot A_{\mu\nu} \right] \psi \quad (1-1)$$

where  $g_A$  was of the order of  $g_\rho$ , the  $\rho$ -nucleon coupling constant. ( $\psi$  is the nucleon field operator,  $A_\mu$  is the axial-vector field operator and

$$A_{\mu\nu} = \partial_\nu A_\mu - \partial_\mu A_\nu$$

( $m$  is the nucleon mass.) Charge-conjugation invariance is violated in eq. 1-1 because  $\bar{\psi} \gamma_5 \gamma^\mu \psi$  is even under  $C$  whereas  $\bar{\psi} \gamma_5 \sigma^{\mu\nu} \psi$  is odd. Parity is manifestly conserved by  $\mathcal{L}^{int}$  so CP is violated. Sudarshan used an SU(4) scheme to relate meson-baryon coupling constants, and specifically, to relate the  $\rho$ -nucleon coupling constant to the  $A_1$ -nucleon coupling constant. He introduced C-violation in the  $A_1$ -nucleon coupling by setting  $F_A = \pm g_A$ , where  $F_A/2m_A = g_A/4m$ . ( $m_A$  is the  $A_1$  mass.) This had the advantage of providing an additional factor of  $\sqrt{2}$  is the ratio of  $A_1$ -nucleon to  $\rho$ -nucleon couplings, such that

$$g_A = (5/3\sqrt{2}) g_\rho = 1.18 g_\rho \quad (1-2)$$

giving a V-1.18A rule for the hadronic weak interaction, the ratio desired at the time. This also gave CP violation in the strong interaction.

We became interested in this theory because of the implications for the strong nucleon-nucleon (NN) interaction. With CP violation, the assumption that CPT is good yields T-violation, and time-reversal invariance was thought to be good to at least 1/3% among strongly interacting particles. However we carried out calculations using Sudarshan's Lagrangian (eq. 1-1) within the framework of a one-boson-exchange (OBE) nucleon-nucleon potential model<sup>2)</sup>; T-violation occurred due to the exchange of the  $A_1$  between the nucleons with  $g_A$  coupling at one vertex and  $f_A$  coupling at the other. This process is illustrated in fig. 1. (We shall refer to this T-violating NN model henceforth as the BG model.) To our surprise, we found that due to the large mass of the  $A_1$  and the consequent short range of the  $A_1$ -nucleon exchange potential, T-violation stayed within the bounds of strong-interaction experimental tests<sup>3)</sup>. These tests included comparisons of relative cross sections in  $p + {}^{25}\text{Mg} \rightleftharpoons d + {}^{24}\text{Mg}$ ,  $T_p = 15$  MeV,  $T_d = 10$  MeV (ref. 4), measurements of polarization minus asymmetry ( $P - \mathcal{A}$ ) in nucleon-nucleon scattering up to 635 MeV in pp and np scattering<sup>3</sup>, and a measurement of  $P_A - P_B$  (essentially a triple-scattering experiment) in pp scattering at 430 MeV. More strict tests of T-asymmetry in hadronic reactions have since appeared, including measurements of  $P$  and  $\mathcal{A}$  in np scattering at 500 and 600 MeV (refs. 3,5) and a very recent measurement of  $P - \mathcal{A}$ , also in np scattering, at 635 MeV (ref. 6). Our calculations using Sudarshan's Lagrangian still get under these

tests if the T-asymmetric part of the  $A_1$ -exchange potential is reduced to 1/3 of the value used in our early work<sup>2)</sup>; indeed, this is exactly how much it should be reduced, because originally we related  $g_A$  to a value of  $g_\rho^2$  which was two times too large (we used the OBE BG-model value of  $g_\rho^2$ , 1.22, instead of the experimental value, 0.5 - 0.7) and also we used too large a value for  $g_A$  as a consequence of the way we defined it in the presence of a short-range potential cutoff factor.<sup>7)</sup> Thus it appears that Sudarshan's hypothesis of strong-interaction CP-violation is not ruled out as far as low-and medium-energy strong-interaction hadronic measurements are concerned. (For a very nice review of experimental tests of T-symmetry, see the article by Richter.<sup>8)</sup>

Nevertheless, the Sudarshan hypothesis (eq. 1-1) is almost certainly wrong; this is not because of hadronic tests, but because of an electromagnetic test: the electric dipole moment of the neutron. This quantity has recently been measured by Ramsey and collaborators<sup>9)</sup> to be less than  $3 \times 10^{-24}$  e-cm. Now, a non-vanishing electric dipole moment  $p_n$  requires that both parity and time-reversal invariance be violated; parity violation alone is sufficient to reduce  $p_n$  to  $10^{-6} \mu_n$ , where  $\mu_n$  is the neutron's magnetic dipole moment. But Ramsey's experiment puts  $p_n \sim 10^{-10} \mu_n$ , so the T-asymmetric part of the amplitude must not exceed one part in  $10^4$ . This rules out the Sudarshan hypothesis, and with it, any possibility of T-asymmetry in hadronic reactions as strong as the BG-model predictions.<sup>3)</sup>

The predictions of the BG model for the relative magnitudes of  $P - A$ ,  $P_A - P_B$ , and other time-asymmetric observables are still useful, however. The reason is that the BG T-violating mechanism is of such short range

that it predicts nearly the same angular dependence for  $t(\theta)$ , the parity and isospin-conserving, T-violating NN Wolfenstein amplitude, as does any other short-range T-asymmetric force. Thus the BG model's predictions for the relative angular distributions of  $P - A$ ,  $P_A - P_B$ , etc. are nearly the same as those of any other NN model with a short-range time-irreversible force, provided that such other model fits the T-reversible NN data.

The reason that the BG prediction for the angular dependence of  $t(\theta)$  is nearly the same as that of any other short-range T-violating model is simply that the T-violation acts mostly in just the lowest permitted angular momentum state. This gives  $t(\theta)$  the angular dependence of the first term in its partial-wave expansion (see Appendix B, eq. B36 and Appendix C, eq. C6, for this expansion for np and pp scattering, respectively). The unique angular dependence of  $t(\theta)$  for suitably short-range T-violation is analogous to the unique angular dependence for the spin 0-spin 0 scattering amplitude  $f(\theta)$  for suitably short-range (central) forces;

$$f(\theta) = k^{-1} [\exp(i\delta_0)] \sin \delta_0 P_0(\cos \theta)$$

and is constant in  $\theta$  for any short-range model.

We focussed on this short-range T-violating universality of the BG model and decided to optimize the model by requiring that T-asymmetry prevail in only the lowest-permitted partial wave ( $j = 1$  in np scattering,  $j = 2$  in pp scattering), and by setting the five T-symmetric amplitudes to the exact experimental predictions obtained from phase-shift analysis of NN data. (The BG model does not fit the  $I = 0$  phase shifts too well at higher energies.) The T-violation is parameterized by a new phase parameter,  $\lambda_j$ ,

which we take to be infinitesimal so as to get under the recent upper limits set by the electric-dipole measurement, and also to avoid throwing off the T-symmetric predictions of the phase shift analysis. We dubbed this model the "zero-range" model.

Preliminary predictions of this model were compared with BG predictions in a previous publication<sup>10)</sup> and are reproduced in fig. 2. One can see that at 425 MeV, predictions of the zero-range model agree pretty well with those of the BG model in the case of pp scattering. In np scattering the agreement is not as good at 425 MeV, but is very good at lower energies. This is illustrated in a later section. The advantage to the experimentalist of model-independent predictions is obvious. For example, in pp scattering, a measurement of  $P_A - P_B$  in the range  $50^\circ$  to  $90^\circ$  at 425 MeV will not be sensitive to short-range time-irreversible forces (although it might be sensitive to long-range T-violating forces).

A limitation of the zero-range model is that it does not predict the absolute magnitude of  $t(\theta)$ , only its relative angular dependence. Thus the model is really a constrained phase-shift analysis, with the magnitude of  $\lambda_1$  ( $\lambda_2$ ) to be filled in by an appropriate np (pp) experiment. In the following sections we describe the model in detail, and provide predictions for pp and np  $P - Q$  and  $P_A - P_B$  at several energies between 50 and 425 MeV. Four appendices provide more detail on properties of the scattering matrix, methods of parameterizing the S-matrix, adding in the Coulomb interaction, and relating  $P_A - P_B$  to the Wolfenstein amplitudes.

## 2. The two-nucleon scattering formalism

In this section we sketch the mathematical formalism for two-nucleon scattering, and emphasize those aspects pertinent to time-reversal. For simplicity, we develop some of the formalism in the regime of non-relativistic scattering but the formulas used for our ultimate predictions are fully relativistic.

Consider nucleon "a" impinging on target nucleon "b". In the center-of-mass system, the NN wavefunction  $\psi$  satisfies the Schrodinger equation

$$-\left(\hbar^2/m\right) \nabla^2 \psi + V\psi = i\hbar \partial\psi/\partial t$$

where  $\psi$  is a function of the time  $t$  and the di-nucleon separation distance  $\underline{r}$ . At a very early time,  $t_i$ , we assume the system to be in a plane-wave state

$$\phi_i = e^{-iE_i t/\hbar} e^{i\underline{k}_i \cdot \underline{r}} \underline{\chi}_i$$

where  $\underline{\chi}_i$  is a four-component non-relativistic spinor. It might take the form

$$\chi_i = \begin{pmatrix} 1 \\ 0 \\ 0 \\ 0 \end{pmatrix} = \chi_{1,1}$$

for combined total spin  $S = 1$  and z-component  $m_S = 1$ ,

$$\chi_2 = \begin{pmatrix} 0 \\ 1 \\ 0 \\ 0 \end{pmatrix} = \chi_{1,0}$$

for  $S = 1$ ,  $m_s = 0$ , and so on. (See definitions for the  $\chi_{S,m_s}$  in Appendix B, following eq. B1.)

Then from standard scattering theory one knows that as the time  $t_i$  approaches  $-\infty$  and the separation distance approaches  $\infty$  (on a scale of nuclear dimensions)

$$\lim_{\substack{t_i \rightarrow -\infty \\ r \rightarrow \infty}} \psi = e^{-iE_i t/k} \left[ e^{i\mathbf{k}_i \cdot \mathbf{r}} + r^{-1} e^{i\mathbf{k}_i \cdot \mathbf{r}} M(\theta, \phi) \right] \chi_i$$

where  $\chi_i$  is the initial spin configuration and  $M$  is the  $4 \times 4$  scattering matrix.  $M$  is a function of the energy  $E$  and the center-of-mass scattering angles  $\theta$  and  $\phi$ . Standard formulas relate  $M$  to scattering observables; for example, the unpolarized differential cross section  $I_0$  is simply

$$I_0 = \frac{1}{4} \text{Tr } M^\dagger M.$$

Now if the interaction  $V$  is independent of the external orientation of the scattering particles, then total angular momentum  $j$  is conserved and  $M$  must take the form

$$\begin{aligned}
 M = & A + B_1 \sigma_p^a + B_2 \sigma_q^a + B_3 \sigma_n^a \\
 & + C_1 \sigma_p^b + C_2 \sigma_q^b + C_3 \sigma_n^b \\
 & + D_{11} \sigma_p^a \sigma_p^b + D_{12} \sigma_p^a \sigma_q^b + D_{13} \sigma_p^a \sigma_n^b \\
 & + D_{21} \sigma_q^a \sigma_p^b + D_{22} \sigma_q^a \sigma_q^b + D_{23} \sigma_q^a \sigma_n^b \\
 & + D_{31} \sigma_n^a \sigma_p^b + D_{32} \sigma_n^a \sigma_q^b + D_{33} \sigma_n^a \sigma_n^b,
 \end{aligned} \tag{2-1}$$

where  $A$ , the  $B_i$ , the  $C_j$ , and the  $D_{ij}$  are each functions of  $k_i^2 = k_f^2 = k^2$  and  $\hat{k}_f \cdot \hat{k}_i = \cos \theta$ , with  $\hat{k}_f$  the final center-of-mass momentum;  $|\hat{k}_f| = |\hat{k}_i|$  because of energy conservation;  $\sigma_p^a = \hat{\sigma}^a \cdot \hat{p}$ ,  $\sigma_q^b = \hat{\sigma}^b \cdot \hat{q}$ , etc. where  $\hat{\sigma}^a$  and  $\hat{\sigma}^b$  are the Pauli spin matrices for nucleons "a" and "b", and  $\hat{p}$ ,  $\hat{q}$ , and  $\hat{n}$  are an orthogonal set of unit vectors related to the initial and final momenta by

$$\hat{p} = \hat{k}_f + \hat{k}_i$$

$$\hat{q} = \hat{k}_f - \hat{k}_i$$

and

$$\hat{n} = \hat{k}_i \times \hat{k}_f.$$

Carets denote vectors of unit length.

Although conservation of total angular momentum places by far the most severe constraint on the M-matrix, other conservation (or symmetry) laws also limit M. Parity conservation, which we shall assume throughout this paper, limits M to the form

$$\begin{aligned}
 M = & A + B_3 \sigma_n^a + C_3 \sigma_n^b + D_{11} \sigma_p^a \sigma_p^b \\
 & + D_{12} \sigma_p^a \sigma_g^b + D_{21} \sigma_g^a \sigma_p^b \\
 & + D_{22} \sigma_g^a \sigma_g^b + D_{33} \sigma_n^a \sigma_n^b.
 \end{aligned}
 \tag{2-2}$$

For later convenience, we re-express M in an equivalent set of amplitudes a, c, f, g, h, m, t, and u. All are functions of  $k^2$  and  $\cos \theta$ , of course.

$$\begin{aligned}
 M = & a + c(\sigma_n^a + \sigma_n^b) + f(\sigma_n^a - \sigma_n^b) \\
 & + (g+h)\sigma_p^a \sigma_p^b + (g-h)\sigma_g^a \sigma_g^b \\
 & + m\sigma_n^a \sigma_n^b + t(\sigma_g^a \sigma_p^b + \sigma_p^a \sigma_g^b) \\
 & + u(\sigma_g^a \sigma_p^b - \sigma_p^a \sigma_g^b).
 \end{aligned}
 \tag{2-3}$$

In the case of pp scattering, the fact that the particles are identical eliminates two more terms in M; it then takes the form

$$\begin{aligned}
 M = & a + c(\sigma_n^a + \sigma_n^b) + (g+h)\sigma_p^a \sigma_p^b \\
 & + (g-h)\sigma_g^a \sigma_g^b + m\sigma_n^a \sigma_n^b \\
 & + t(\sigma_g^a \sigma_p^b + \sigma_p^a \sigma_g^b).
 \end{aligned}
 \tag{2-4}$$

(Note that this reduction of M occurs because the protons are identical, not because of the Pauli principle. An M-matrix for identical bosons is similarly reduced.) In the case of np scattering, conservation of isobaric spin also leads to the form of eq. 2-4.

If the interaction is invariant under time-reversal, then one more term falls out and M becomes

$$\begin{aligned}
 M = & a + c(\sigma_n^a + \sigma_n^b) + (g+h)\sigma_p^a \sigma_p^b \\
 & + (g-h)\sigma_p^a \sigma_p^b + m\sigma_n^a \sigma_n^b.
 \end{aligned}
 \tag{2-5}$$

(This is the set of Wolfenstein amplitudes used by MacGregor, Moravcsik and Stapp<sup>11</sup>.) The details of the effect of each symmetry condition on M are given in Appendix A.

Now the quantity of interest to us for this paper is  $t(\theta)(\sigma_q^a \sigma_p^b + \sigma_p^a \sigma_q^b)$ , that part of the total scattering amplitude which is not time-reversal invariant. We will first relate  $t(\theta)$  to some experiments which reveal T-asymmetry, and then we will relate  $t$  to the scattering phase shifts.

The classical test<sup>12</sup> for T-noninvariance is the measurement  $P - a$ , the polarization minus the asymmetry. In terms of the Wolfenstein amplitudes,

$$I_0 (P - a) = 8 \text{Im } h^* t, \quad (2-6)$$

so vanishing  $t$  requires vanishing  $P - a$ . Experimentally, one may measure  $P$  by scattering an unpolarized beam of nucleons off a target of unpolarized nucleons as depicted in fig. 3A. Ordinarily the scattered beam becomes polarized (but only in the direction normal to the scattering plane if parity is good), and this polarization can be measured by a second scattering (off carbon, for example). Recalling that the beam particles are designated "a", the formula for the polarization of the scattered beam at an angle  $\theta$  is

$$I_0 P = \frac{1}{4} \text{Tr} (M^\dagger \sigma_n^a M).$$

To measure the asymmetry,  $a$ , one may scatter a beam of polarized protons to the left and to the right off an unpolarized target, as shown in fig. 3B. If the initial beam is 100% polarized, normal to the scattering plane (when parity is good, only the normal component contributes to the asymmetry) then the asymmetry  $a$  is

$$a = (\sigma_L - \sigma_R) / (\sigma_L + \sigma_R)$$

where  $\sigma_L$  and  $\sigma_R$  are relative cross sections for left and right-scattering, respectively. In terms of the M-matrix,

$$I_0 a = \frac{1}{4} \text{Tr} (M^\dagger M \sigma_n^a).$$

If we express M in the form of eq. 2-4, then after a little matrix algebra we find that

$$I_0 (P - a) = 8 \text{Im} h^* t$$

as mentioned previously; evaluation of the traces is straightforward using the relations

$$\sigma_p \sigma_q = i \sigma_n \quad (P, q, n \text{ cyclic})$$

and

$$\text{Tr} 1 = 4.$$

The other experiment cited for detecting T-noninvariance is  $P_A - P_B$ . It was invented by Pondrom<sup>13)</sup> and is sketched in fig. 4 as it appears in the center-of-mass system. It consists of two measurements, which in the figure are labelled A and B. (Drawing B' is just a rotation of drawing B.) For measurement A, one takes a beam of polarized protons moving in the di-

rection  $\underline{k}_i$  and measures the polarization along an axis  $\underline{A}$  of those protons scattering into direction  $\underline{k}_f$ . Call this component<sup>51</sup> of final polarization,  $P_A$ . The initial polarization axis and  $\underline{A}$  are both to lie in the scattering plane. (We take  $P = 100\%$  for simplicity.) The angles  $\chi_i$  and  $\chi_f$  are free to be chosen by the experimentalist, but there is an optimal choice which will be apparent shortly.

For measurement B, one arranges the projectile beam to be moving in the direction  $-\underline{k}_f$ , and to have polarization (100% for simplicity) in the direction opposite to axis  $\underline{A}$  of part A. One considers particles which scatter into the direction  $-\underline{k}_i$  and measures the component of polarization along an axis  $\underline{B}$ , where  $\underline{B}$  is directed opposite to the initial polarization axis of the first experiment. Call this component of polarization  $P_B$ . Note that  $\underline{A}$  and  $\underline{B}$  lie in the scattering plane, just as their counterparts in experiment A.

One now compares  $P_A$  with  $P_B$ . It happens that if  $P_B = P_A$ , T is good, whereas if  $P_B \neq P_A$ , T is bad. The explicit formula for  $P_A - P_B$  is

$$I_0(P_A - P_B) = \sin(\chi_i + \chi_f) \cdot 8 \operatorname{Re} g^* t. \quad (2-7)$$

The derivation of this formula is given in Appendix D. One sees that an optimal choice for  $\chi_i + \chi_f$  is  $\pm 90^\circ$ .

We now consider the expansion of  $t(\theta)$  in terms of partial-wave scattering amplitudes; this is of interest when considering the T-asymmetric OBEP model<sup>2)</sup> (BG model) and leads to the definition of our zero-range model.

As we show in Appendix B, eq. B35,

$$t(\theta) = (4k)^{-1} \sum_{j=1}^{\infty} (2j+1) [j(j+1)]^{-\frac{1}{2}} P_j^{(1)}(\cos \theta) \\ \cdot [ \langle j, j-1, 1 | T | j, j+1, 1 \rangle \\ - \langle j, j+1, 1 | T | j, j-1, 1 \rangle ] \quad (2-8)$$

for np scattering, where  $P_j^{(1)}$  is the associated Legendre polynomial with magnetic quantum number  $m = 1$ , and  $k$  is the center-of-mass momentum of either nucleon. We stress that this expression is fully relativistic.

The matrix elements of  $T$  in eq. 2-8 are the off-diagonal elements of the  $2 \times 2$   $T$ -matrix for fixed  $j$ ,  $s = 1$ , and  $\ell = j \pm 1$ , which we denote  $T_{j\pm}$ .  $T_{j\pm}$  is related to the  $S$ -matrix for this subspace by the usual formula;

$$T_{j\pm} = (S_{j\pm} - 1)/2i. \quad (2-9)$$

We find a convenient parameterization of the  $S$ -matrix to be<sup>10)</sup>

$$S_{j\pm} = e^{i\delta_j} e^{i\epsilon_j} e^{2i\lambda_j} e^{i\epsilon_j} e^{i\delta_j} \quad (2-10)$$

where

$$\sigma_2 = \begin{pmatrix} \delta_{j,j-1} & 0 \\ 0 & \delta_{j,j+1} \end{pmatrix}$$

$$\sigma_1 = \begin{pmatrix} 0 & \epsilon_j \\ \epsilon_j & 0 \end{pmatrix} = \epsilon_j \sigma_1$$

and

$$\lambda_j = \begin{pmatrix} 0 & -i\lambda_j \\ i\lambda_j & 0 \end{pmatrix} = \lambda_j \sigma_2$$

In terms of this choice of phase parameters,  $t(\theta)$  takes the form

$$t(\theta) = (2k)^{-1} \sum_{j=1}^{\infty} (2j+1) [j(j+1)]^{-\frac{1}{2}} \times P_j^{(1)}(\cos \theta) \sin 2\lambda_j \exp i(\delta_{j,j-1} + \delta_{j,j+1}) \quad (2-11)$$

as shown in Appendix B, eq. B36.

In the case of proton-proton scattering, the Pauli exclusion principle forbids spin triplet-even states and singlet-odd states, and the appropriate expansion for  $t$  is

$$t(\theta) = k^{-1} \sum_{j \text{ even}} (2j+1) [j(j+1)]^{-\frac{1}{2}} P_j^{(1)}(\cos \theta) \\ \times \sin 2\lambda_j \exp i (\delta_{j,j-1}^N + \phi_{j-1} + \delta_{j,j+1}^N + \phi_{j+1}) \quad (2-12)$$

where the  $\delta_{j\ell}^N$  are the "nuclear bar" phase shifts and  $\phi_\ell$  is the Coulomb phase shift<sup>14)</sup> for the  $\ell^{\text{th}}$  partial wave. Eq. 2-12 is derived in Appendix C.

To help visualize the effect of the several invariance conditions on transitions between different angular momentum states, we illustrate classes of transitions in fig. 5. The first two columns concern np scattering, the third pp scattering. In each column we list as initial and final states, all possible angular momentum states through  $j = 2$ . Allowed transitions are indicated by a line connecting the states. In the first column one sees the effect of invariance of the interaction under space rotation and space inversion of the initial and final scattering states (transitions are only allowed between states of the same T and parity). In the second column one sees the effect of imposing invariance under rotations in isospin space as well (the initial and final states must have the same I). E.g.,  $^1P_1 \nrightarrow ^3P_1$  and  $^1D_2 \nrightarrow ^3D_2$  transitions are now forbidden.

The effect of imposing time-reversal invariance is more subtle. It is not that any transitions are forbidden; rather, the S- (and T-) matrices are required to be symmetric. Thus, when time-reversal invariance is good,  $\langle ^3S_1 | T | ^3D_1 \rangle = \langle ^3D_1 | T | ^3S_1 \rangle$ ,  $\langle ^3P_2 | T | ^3F_2 \rangle = \langle ^3F_2 | T | ^3P_2 \rangle$ , etc. This is why  $t(\theta)$  is a weighted sum over  $j$  of the difference between each pair of off-diagonal transitions.

In the case of pp scattering, half the angular momentum states disappear because of the Pauli exclusion principle. Thus the lowest j-value where time-reversal noninvariance can show up is  $j = 2$ . This has the result of severely reducing the effect of any T-violating forces on pp observables if the T-asymmetry is of short range and the energy is low.

### 3. The zero-range model

Bryan and Gersten observed that T-violation in the BG one-boson-exchange model is much stronger in the  $j = 1$  state than in the higher-j states.<sup>2)</sup> This can be seen in fig. 6, wherein is plotted  $\lambda_j$  for the BG model vs.  $T_{lab}$ , for  $j = 1$  through 4 and  $T_{lab}$  from 0 to 635 MeV. It is readily apparent why T-asymmetry is much more pronounced in the low-j states; it is caused by the exchange of an  $A_1$  meson with an assigned mass of  $1070 \text{ MeV}/c^2$ , and the short range of such a heavy meson naturally favors exchange between states of low orbital angular momentum. (The derivative coupling of the  $A_1$  at one nucleon vertex makes the range of the potential even shorter; see eq. 1-1.) It follows then that  $t(\theta)$  receives its dominant contribution from transitions involving the lowest j-value. So from eq. 2-11 one sees that for np scattering,  $t(\theta)$  is predominantly given by

$$(3\sqrt{2}/4k) \{ \exp i [ \delta(^3S_1) + \delta(^3D_1) ] \} \sin 2\lambda_1 \sin \theta \quad (3-1)$$

while for pp scattering (eq. 2-12)  $t(\theta)$  is largely given by

$$(5\sqrt{6}/2k) \{ \exp i [ \delta^N(^3P_2) + \phi_1 + \delta^N(^3F_2) + \phi_3 ] \} \\ \times \sin 2\lambda_2 \sin \theta \cos \theta. \quad (3-2)$$

(As it happens,  $t(\theta)$  for pp scattering is even better approximated by 3-2 than is the np  $t(\theta)$  by 3-1; this is because the pp  $t(\theta)$  receives contributions only from  $\lambda_2, \lambda_4, \lambda_6, \dots$  and this is a much more rapidly converging series than is  $\lambda_1, \lambda_2, \lambda_3, \dots$ , as may be seen in fig. 6.)

It occurred to us that it might be interesting to see what the prediction for time-reversal asymmetry would be in the limit where only the lowest-allowed j-value transitions would be permitted to contribute. Such a model would correspond to T-violating exchange mechanisms of extremely short range (especially in np scattering; not quite so short in pp scattering). We stress that such a model would predict a universal angular dependence for  $t(\theta)$ , true for any short-range T-asymmetry model, no matter what the mechanism, because the Legendre polynomial expansion of  $t(\theta)$  would have only the leading term (variation in the angular dependence of  $t(\theta)$  for different models is of course due to different ratios of  $\lambda_1:\lambda_2:\lambda_3:::$ ). As a further refinement in the zero-range model the T-symmetric amplitudes a, c, g, h, and m (eq. 2-4) could be taken from accurate phase-shift analysis of the nucleon-nucleon data itself, rather than from a given theoretical model like the BG model (which does not fit the  $l = 0, \lambda = 2$  experimental phase parameters above 200 MeV as well as we would like). Thus predictions for the NN experimental observables would also be generically correct for any model of short-range T-violation as far as angular dependence is concerned. For example,  $I_0(\theta)(P - \mathcal{A}) = 8 \text{Im}[h^*(\theta)t(\theta)]$ , so with  $I_0(\theta)$  and  $h(\theta)$  given by experiment, and  $t \propto \sin \theta$  (np case) or  $\sin \theta \cos \theta$  (pp case), the angular dependence of  $P - \mathcal{A}$  is completely determined.<sup>§2</sup>

The disadvantage of this model is that the magnitude of  $t(\theta)$ , and hence the observables, is unknown. Thus it yields only relative values for the observables. But such information can still be of great value. For example, consider the measurement of  $P_A - P_B$  in pp scattering at 430 MeV. Data was published for only one angle<sup>13)</sup>; this point is plotted in fig. 2a. The BG model prediction is plotted on the same graph and it can be seen that a measurement in the range of  $10^\circ$ - $30^\circ$  cm, or  $120^\circ$ - $160^\circ$  cm would have been much more valuable in testing for short-range time-irreversibility, had such a measurement been able to be made to the same degree of accuracy.

Accordingly we decided to proceed with the zero-range model and carry out calculations. We first present the details of the model, and then the experimental predictions. The model consists of assigning to  $t(\theta)$  just the lowest term in the Legendre expansion, with  $\lambda_1$  (np case) or  $\lambda_2$  (pp case) taken to be infinitesimal. In this fashion we do not throw off the predictions of the T-symmetric amplitudes. Thus, for np scattering, we set

$$t(\theta) = \lambda_1 (3\sqrt{2}/2k) \{ \exp i [\delta(^3S_1) + \delta(^3D_1)] \} \sin \theta$$

and for pp scattering, we set

$$t(\theta) = \lambda_2 (5\sqrt{6}/k) \{ \exp i [\delta^N(^3P_2) + \phi_1 + \delta^N(^3F_2) + \phi_3] \} \\ \times \sin \theta \cos \theta.$$

The values for  $\delta(^3S_1)$ ,  $\delta(^3D_1)$ ,  $\delta(^3P_2)$ , and  $\delta(^3F_2)$  in these expressions are taken directly from experiment, in the form of the Arndt-MacGregor-Wright phase-shift analyses of the NN data<sup>15)</sup> (MAW-X), available at several energies up to 425 MeV. The five remaining, T-symmetric amplitudes  $a(\theta)$ ,  $c(\theta)$ ,  $g(\theta)$ ,  $h(\theta)$ , and  $m(\theta)$  are also directly computed from the MAW-X phase shifts. Formulas for the expansion of these five amplitudes in terms of the phase parameters can be found, e.g. in the review articles by MacGregor, Moravcsik, and Stapp<sup>16)</sup> and Hoshizaki<sup>17)</sup>. Coulomb corrections in the case of pp scattering are handled in the usual way, as e.g. in ref. 14 and Appendix C.

We present graphs of our calculated observables in figs. 7 and 8 for pp and np scattering, respectively.  $(P - Q)/\lambda_2$  and  $(P_A - P_B)/\lambda_2$  appear in fig. 8, and  $(P - Q)/\lambda_1$  and  $(P_A - P_B)/\lambda_1$  appear in fig. 9. Computations were carried out at 50, 95, 142, 210, 330, and 425 MeV. An absolute value for any of the plotted observables can be arrived at by multiplying the value on the graph by  $\lambda_1(\lambda_2)$  in the case of np (pp) scattering. Alternatively, if a measurement is performed, then  $\lambda_1(\lambda_2)$  can be determined by dividing the np (pp) measurement by the corresponding plotted value.

#### 4. Discussion

It is of interest to compare the zero-range model's predictions for pp and np T-asymmetric observables with corresponding predictions of the BG one-boson-exchange model. This affords some insight into how model-independent the zero-range predictions are. The BG predictions for pp and np observables are graphed in figs. 9 and 10 respectively. On comparing

the np observables for the two models, one sees that the predictions for  $P - Q$  agree only roughly at 425 MeV, and that they agree much better at 145 and 50 MeV (figs. 10a and 8a). The same is true of the BG and zero-range model's np predictions for  $P_A - P_B$  (figs. 10b and 8b).

In the case of pp scattering, the agreement between the zero-range and BG model's predicted observables is quite good at all energies up through 425 MeV. The better agreement in the pp case is due to the more rapid vanishing of the BG  $\lambda_j$ 's with increasing  $j$  ( $\lambda_2, \lambda_4, \lambda_6, \dots$ ) as shown in fig. 6, and the better fit of the  $I = 1$  BG phase parameters to experiment<sup>2)</sup>. Thus, while we hold certain reservations about either model's predictions for np T-asymmetric observables (is it valid to neglect isospin-nonconservation<sup>53</sup>?) we feel confident that the models' predictions for pp time-irreversible observables accurately reflect the effect of short-range T-violations whatever the cause.

The BG model affords some insight into the relative magnitude of np and pp measurements of T-violation, and also their energy-dependence. Clearly a given short-range T-asymmetric force produces a much larger  $\lambda_1$  than  $\lambda_2$ , as illustrated in fig. 6.<sup>54</sup> Correspondingly, time-irreversibility will show up more strongly in np scattering, where  $\lambda_1$  contributes, than in pp scattering where it does not.

It is also clear from the BG predictions (fig. 6) that  $\lambda_j$  increases sharply with energy. This would appear to be true of any short-range T-irreversible force. Thus T-violation for such a force should be more apparent at higher energies. However one must fold in the effect of the T-conserving amplitudes as well for any given observable. For example, in

pp  $P_A - P_B$ , the amplitude  $g(\theta)$  has the effect of enhancing the observable at 50 MeV for a given  $\lambda_2$ , as may be seen from fig. 7b.

We would like to thank Professor E. C. G. Sudarshan for interesting conversations about this work. One of us (R. A. B.) would also like to thank Dr. M. Simonius for stimulating discussions on the role of isospin violation in time-irreversible nuclear forces. This author also gratefully acknowledges the kind hospitality provided at the Research Institute for Theoretical Physics, Helsinki, Finland, from Sept 1974-Sept 1975, by Professor A. M. Green and the staff while he was visiting that institution under the kind auspices of the Nordic Institute for Theoretical Atomic Physics (NORDITA).

Appendix A. General form of the M-matrix

Consider nucleon a scattering off nucleon b, as depicted in fig. 11a. Here  $\underline{p}_i$ ,  $\pi_i$ ,  $\underline{n}_i$ , and  $\nu_i$  are the initial three-momentum and intrinsic spin of nucleons a and b, respectively, and  $\underline{p}_f$ ,  $\pi_f$ ,  $\underline{n}_f$ , and  $\nu_f$  are the corresponding quantities in the final state. The initial and final center-of-mass momenta are defined to be

$$\underline{k}_i = \frac{1}{2}(\underline{p}_i - \underline{n}_i)$$

and

$$\underline{k}_f = \frac{1}{2}(\underline{p}_f - \underline{n}_f),$$

respectively. Then if the interaction is invariant under the rotation in space of the nucleons' initial and final three-momenta and intrinsic spins, the M-matrix must take the form of eq. 2-1 in the text.

Consider next the effect on the initial and final momenta and spins, of space-reflection through the origin of coordinates. The momenta reverse direction while the spins remain unchanged. This is illustrated in fig. 11b; the space-reflected momentum and spin symbols are underlined. If we now require that the interaction be invariant under space-reflection, half the amplitudes in M (eq. 2-1) vanish. Specifically, invariance under space-reflection means that

$$\begin{aligned} \chi_{\pi_f}^{a\dagger} \chi_{\nu_f}^{b\dagger} M(\underline{k}_f, \underline{k}_i) \chi_{\pi_i}^a \chi_{\nu_i}^b \\ = \chi_{\pi_f}^{a\dagger} \chi_{\nu_f}^{b\dagger} M(\underline{k}_f, \underline{k}_i) \chi_{\pi_i}^a \chi_{\nu_i}^b \end{aligned} \quad (A1)$$

where the  $\chi^a$  and  $\chi^b$  are two-component spinors for nucleons a and b. Since under space reflection the spins do not change but the momenta reverse direction, eq. A1 may be written

$$\begin{aligned} \chi_{\pi_f}^{a\dagger} \chi_{\nu_f}^{b\dagger} M(-\underline{k}_f, -\underline{k}_i) \chi_{\pi_i}^a \chi_{\nu_i}^b \\ = \chi_{\pi_f}^{a\dagger} \chi_{\nu_f}^{b\dagger} M(\underline{k}_f, \underline{k}_i) \chi_{\pi_i}^a \chi_{\nu_i}^b \end{aligned}$$

or, in general

$$M(-\underline{k}_f, -\underline{k}_i) = M(\underline{k}_f, \underline{k}_i). \quad (\text{A2})$$

It is now an easy matter to determine which terms in eq. 2-1 drop out.

The arguments of the amplitudes  $A$ ,  $B_i$ ,  $C_j$ , and  $D_{ij}$  are  $\underline{k}_i \cdot \underline{k}_i$  and  $\underline{k}_i \cdot \underline{k}_f$ , hence remain unchanged under space-reflection. However

$$\underline{P} = \underline{k}_f + \underline{k}_i = -\underline{P}$$

and 
$$\underline{Q} = \underline{k}_f - \underline{k}_i = -\underline{Q}$$

$$\underline{n} = \underline{k}_i \times \underline{k}_f = \underline{n}$$

and thus  $\sigma_P^a$ ,  $\sigma_Q^a$ ,  $\sigma_P^b$ ,  $\sigma_Q^b$ ,  $\sigma_P^a \sigma_n^b$ ,  $\sigma_Q^a \sigma_n^b$ ,  $\sigma_n^a \sigma_P^b$ , and  $\sigma_n^a \sigma_Q^b$  change sign.

Hence eq. A2 forces the coefficients of these matrices to vanish. Thus

the most general form for  $M$  under space-rotation and -inversion invariance is

$$\begin{aligned} M = & A + B_3 \sigma_n^a + C_3 \sigma_n^b + D_{11} \sigma_P^a \sigma_P^b \\ & + D_{12} \sigma_P^a \sigma_Q^b + D_{21} \sigma_Q^a \sigma_P^b \\ & + D_{22} \sigma_Q^a \sigma_Q^b + D_{33} \sigma_n^a \sigma_n^b. \end{aligned}$$

A more common choice of amplitudes is such that

$$\begin{aligned}
 M = & a + c(\sigma_n^a + \sigma_n^b) + f(\sigma_n^a - \sigma_n^b) \\
 & (g+h)\sigma_p^a\sigma_p^b + (g-h)\sigma_g^a\sigma_g^b + m\sigma_n^a\sigma_n^b \\
 & + t(\sigma_g^a\sigma_p^b + \sigma_p^a\sigma_g^b) + u(\sigma_g^a\sigma_p^b - \sigma_p^a\sigma_g^b).
 \end{aligned}
 \tag{A3}$$

Consider next the restriction on M if nucleons a and b are indistinguishable particles. Then

$$\begin{aligned}
 & \chi_{\pi_f}^{a\dagger} \chi_{\nu_f}^{b\dagger} M(\tilde{p}_i, \tilde{n}_i, \tilde{p}_f, \tilde{n}_f) \chi_{\pi_i}^a \chi_{\nu_i}^b \\
 & = \chi_{\nu_f}^{a\dagger} \chi_{\pi_f}^{b\dagger} M(\tilde{n}_i, \tilde{p}_i, \tilde{n}_f, \tilde{p}_f) \chi_{\nu_i}^a \chi_{\pi_i}^b,
 \end{aligned}
 \tag{A4}$$

that is, M is invariant if the spins and momenta of nucleons a and b are interchanged. Now relabel the r.h.s. of eq. A4 with a→b and b→a everywhere they appear. The result is that eq. A4 becomes

$$M(\tilde{\sigma}_i^a, \tilde{\sigma}_f^b) = M(\tilde{\sigma}_i^b, \tilde{\sigma}_f^a).
 \tag{A5}$$

where  $M(\tilde{\sigma}_i^b, \tilde{\sigma}_f^a)$  is meant to denote the original M-matrix but with the spin matrices interchanged. (We need no longer indicate the spinors as in eq. A4 as they are now identical on both sides of the equation.) Condition A5 reduces M of eq. A3 to the form

$$\begin{aligned}
 M = & a + c(\sigma_n^a + \sigma_n^b) \\
 & + (g+h)\sigma_p^a\sigma_p^b + (g-h)\sigma_g^a\sigma_g^b \\
 & + m\sigma_n^a\sigma_n^b + t(\sigma_g^a\sigma_p^b + \sigma_p^a\sigma_g^b).
 \end{aligned}
 \tag{A6}$$

Consider finally the effect on the space-reflection and rotation invariant M-matrix (eq. A3) if we require time-reversal symmetry. The time-reversed spins and momenta are defined according to fig. 11c; specifically the time-reversed momenta are

$$\begin{aligned}
 \tilde{p}_i &= -p_f, \\
 \tilde{n}_i &= -n_f, \\
 \text{and } \tilde{p}_f &= -p_i \\
 \tilde{n}_f &= -n_i;
 \end{aligned}$$

the time-reversed spins are defined to be

$$\begin{aligned}
 \tilde{\pi}_i &= -\pi_f \\
 \tilde{\nu}_i &= -\nu_f \\
 \tilde{\pi}_f &= -\pi_i \\
 \text{and } \tilde{\nu}_f &= -\nu_i.
 \end{aligned}$$

Returning to the momenta,

$$\begin{aligned}
 \tilde{k}_i &= \frac{1}{2}(-p_f + n_f) = -k_f \\
 \tilde{k}_f &= \frac{1}{2}(-p_i + n_i) = -k_i
 \end{aligned}$$

so that

$$\underline{p} = \underline{k}_f + \underline{k}_i = -\underline{p}$$

$$\underline{q} = \underline{k}_f - \underline{k}_i = +\underline{q}$$

and

$$\underline{n} = \underline{k}_i \times \underline{k}_f = -\underline{n}$$

Concerning the spins, by  $\pi_i = -\pi_f$  we mean that

$$\chi_{\pi_i} = \chi_{-\pi_f}$$

where

$$\chi_{-\pi_f} = A \chi_{\pi_f}$$

equals a spinor whose spin-expectation value is reversed; i.e.

$$\chi_{-\pi_f}^\dagger \underline{\sigma} \chi_{-\pi_f} = -\chi_{\pi_f}^\dagger \underline{\sigma} \chi_{\pi_f}$$

The operator A which reverses the spin direction is given by

$$A = [\exp(-i \underline{\sigma} \cdot \hat{e}_y \pi/2)] K$$

$$= -i \sigma_2 K$$

$$= \begin{pmatrix} 0 & -1 \\ 1 & 0 \end{pmatrix} K,$$

where  $K$  operates so as to replace everything to its right by the complex conjugate. The operator  $U = -i\sigma_2$  rotates all spins by  $180^\circ$  about the  $y$ -axis, and thus reverses the  $x$ - and  $z$ -components of the spin expectation value.  $K$  affects only the  $y$ -components, reversing the direction. Thus  $-i\sigma_2 K$  reverses the entire spin expectation value.

In general, if  $\chi_\alpha$  and  $\chi_\beta$  are any two two-component spinors, then

$$\begin{aligned} (A\chi_\alpha)^\dagger \underline{\sigma} A\chi_\beta &= (K U \chi_\alpha)^\dagger \underline{\sigma} K U \chi_\beta \\ &= (K \chi_\alpha^\dagger) U^\dagger \underline{\sigma} U K \chi_\beta \end{aligned}$$

(since  $KU = UK$ ).

Now a simple calculation confirms that

$$U^\dagger \underline{\sigma} U = -\sigma_1 \hat{e}_x + \sigma_2 \hat{e}_y - \sigma_3 \hat{e}_z.$$

Meanwhile

$$\begin{aligned} (K \chi_\alpha^\dagger) U^\dagger \underline{\sigma} U (K \chi_\beta) &= \chi_\alpha^T U^\dagger \underline{\sigma} U \chi_\beta^\dagger \\ &= \chi_\beta^\dagger (U^\dagger \underline{\sigma} U)^T \chi_\alpha \end{aligned}$$

where the superscript  $T$  denotes "transpose". Since

$$\begin{aligned} (U^\dagger \underline{\sigma} U)^T &= -\sigma_1 \hat{e}_x - \sigma_2 \hat{e}_y - \sigma_3 \hat{e}_z \\ &= -\underline{\sigma}. \end{aligned}$$

PAGES 31 to 32  
WERE INTENTIONALLY  
LEFT BLANK

$\underline{\sigma}^b$  by  $-\underline{\sigma}^b$ , and  $\underline{p}$  and  $\underline{n}$  by  $-\underline{p}$  and  $-\underline{n}$ , respectively;  $\underline{q}$  remains unchanged.

If we now impose condition A10 on the space-rotation and inversion invariant M-matrix (eq. A3) we find that no constraint is imposed on the coefficients, as these are functions of  $k_i^2 = k_f^2 = k_n^2$  and  $\underline{k}_i \cdot \underline{k}_f = \underline{k}_i \cdot \underline{k}_n$ , but that two spin operators are eliminated; M takes the form

$$\begin{aligned}
 M = & a + c(\sigma_n^a + \sigma_n^b) + f(\sigma_n^a - \sigma_n^b) \\
 & + (g+h)\sigma_p^a \sigma_p^b + (g-h)\sigma_g^a \sigma_g^b \\
 & + m \sigma_n^a \sigma_n^b.
 \end{aligned}
 \tag{A11}$$

Appendix B. Phase-shift expansion of the M-matrix

We present an expansion of the M-matrix of eq. A6 in terms of partial-wave matrix elements of the transition operator T. The symbolic matrix relationship between T and the scattering matrix S is  $T=(S-1)/2i$  for a given partial-wave. We will give the precise relationship in each case as it arises.

Although we will give the T-matrix expansion for one of the six amplitudes in eq. A6, that for  $t(\theta)$ , for the entire M-matrix we prefer to use a different representation, that in which the total spin S (1 or 0) and its z-component  $m_s$  is specified, as in ref. 14. Thus, if  $M_{k_f s_f m_f, k_i s_i m_i}$  is the matrix element for initial center-of-mass momentum  $k_i$ , total two-nucleon spin  $s_i$  and z-component  $m_i$ , with  $k_f$ ,  $s_f$ , and  $m_f$  the corresponding quantities in the final state, invariance under space rotation and particle interchange (or isospin in np scattering) permits one to express M as

$$M = \begin{pmatrix} M_{ss} & 0 & 0 & 0 \\ 0 & M_{1,1} & M_{1,0} & M_{1,-1} \\ 0 & M_{0,1} & M_{0,0} & M_{0,-1} \\ 0 & M_{-1,1} & M_{-1,0} & M_{-1,-1} \end{pmatrix} \quad (B1)$$

where the set of basis vectors  $X_{sm}$  are

$$X_{0,0} = \begin{pmatrix} 1 \\ 0 \\ 0 \\ 0 \end{pmatrix}, \quad X_{1,1} = \begin{pmatrix} 0 \\ 1 \\ 0 \\ 0 \end{pmatrix}, \quad X_{1,0} = \begin{pmatrix} 0 \\ 0 \\ 1 \\ 0 \end{pmatrix} \quad \text{and} \quad X_{1,-1} = \begin{pmatrix} 0 \\ 0 \\ 0 \\ 1 \end{pmatrix}$$

and where we denote the  $M_{k_f s_f m_f, k_i s_i m_i}$  as

$$M_{k_f, 0, 0, k_i, 0, 0} = M(\theta, \phi)_{ss}$$

and

$$M_{k_f, 1, m_f, k_i, 1, m_i} = M(\theta, \phi)_{m_f m_i}$$

Here  $\theta$  and  $\phi$  are the polar and azimuthal angles, respectively, of  $k_f$ ; we choose  $k_i$  to lie along the z-axis.

Invariance of  $M$  under space-reflection puts constraints on the  $M_{m_f m_i}$  such that there are now only six independent elements;

$$M = \begin{pmatrix} M_{ss} & 0 & 0 & 0 \\ 0 & M_{1,1} & M_{1,0} & M_{1,-1} \\ 0 & M_{0,1} & M_{0,0} & -M_{0,-1} \\ 0 & M_{1,-1} & -M_{1,0} & M_{1,1} \end{pmatrix} \quad (\text{B2})$$

We now give the expansion of each of these six elements in terms of partial-wave T-matrix elements, written in the form  $\langle j, l_f, s | T | j, l_i, s \rangle$ , where  $j$  is the total angular momentum both initially and finally (it must be conserved because of space rotational invariance of  $M$ ),  $s$  is the spin angular momentum (conserved only because of parity conservation and the Pauli principle (or isospin conservation)) and  $l_f$  and  $l_i$  are the final and initial orbital angular momenta;  $k$  is the magnitude of  $\underline{k}_f$  and  $\underline{k}_i$ .  $M$  is normalized such that the unpolarized differential cross section

$$I_0 = \frac{1}{4} \text{Tr} M^\dagger M.$$

We stress that these expansions are fully relativistic (one must compute  $k$  relativistically) and are a general result of Lorentz covariance and unitarity of the S-matrix.

$$\begin{aligned}
 M_{1,1} = (2k)^{-1} \sum_j \{ & P_{j-1}(\cos \theta) (j+1) \langle j, j-1, 1 | T | j, j-1, 1 \rangle \\
 & - P_{j-1}(\cos \theta) [j(j+1)]^{1/2} \langle j, j-1, 1 | T | j, j+1, 1 \rangle \\
 & + P_j(\cos \theta) (2j+1) \langle j, j, 1 | T | j, j, 1 \rangle \\
 & - P_{j+1}(\cos \theta) [j(j+1)]^{1/2} \langle j, j+1, 1 | T | j, j-1, 1 \rangle \\
 & + P_{j+1}(\cos \theta) \cdot j \langle j, j+1, 1 | T | j, j+1, 1 \rangle \} .
 \end{aligned}
 \tag{B3}$$

$$\begin{aligned}
 M_{1,0} &= (2k)^{-1} \exp(-i\phi) \\
 &\times \sum_j \left\{ P_{j-1}^{(1)}(\cos\theta) 2^{\frac{1}{2}} \langle j, j-1, 1 | T | j, j-1, 1 \rangle \right. \\
 &\quad + P_{j-1}^{(1)}(\cos\theta) [2(j+1)/j]^{\frac{1}{2}} \langle j, j-1, 1 | T | j, j+1, 1 \rangle \\
 &\quad - P_{j+1}^{(1)}(\cos\theta) [2j/(j+1)]^{\frac{1}{2}} \langle j, j+1, 1 | T | j, j-1, 1 \rangle \\
 &\quad \left. - P_{j+1}^{(1)}(\cos\theta) 2^{\frac{1}{2}} \langle j, j+1, 1 | T | j, j+1, 1 \rangle \right\}.
 \end{aligned}$$

(B4)

$$\begin{aligned}
 M_{1,-1} &= (2k)^{-1} \exp(-2i\phi) \\
 &\times \sum_j \left\{ P_{j-1}^{(2)}(\cos\theta) j^{-1} \langle j, j-1, 1 | T | j, j-1, 1 \rangle \right. \\
 &\quad - P_{j-1}^{(2)}(\cos\theta) [j(j+1)]^{-\frac{1}{2}} \langle j, j-1, 1 | T | j, j+1, 1 \rangle \\
 &\quad - P_j^{(2)}(\cos\theta) [(2j+1)/j(j+1)]^{\frac{1}{2}} \langle j, j, 1 | T | j, j, 1 \rangle \\
 &\quad - P_{j+1}^{(2)}(\cos\theta) [j(j+1)]^{-\frac{1}{2}} \langle j, j+1, 1 | T | j, j-1, 1 \rangle \\
 &\quad \left. + P_{j+1}^{(2)}(\cos\theta) (j+1)^{-1} \langle j, j+1, 1 | T | j, j+1, 1 \rangle \right\}.
 \end{aligned}$$

(B5)

$$\begin{aligned}
 M_{0,1} &= (2k)^{-1} \exp(i\phi) \\
 &\times \sum_j \left\{ -P_{j-1}^{(1)}(\cos\theta) 2^{1/2} (j+1) j^{-1} \langle j, j-1, 1 | T | j, j-1, 1 \rangle \right. \\
 &+ P_{j-1}^{(1)}(\cos\theta) [2(j+1)/j]^{1/2} \langle j, j-1, 1 | T | j, j+1, 1 \rangle \\
 &+ P_j^{(1)}(\cos\theta) 2^{1/2} [(2j+1)/j(j+1)] \langle j, j, 1 | T | j, j, 1 \rangle \\
 &- P_{j+1}^{(1)}(\cos\theta) [2j/(j+1)]^{1/2} \langle j, j+1, 1 | T | j, j-1, 1 \rangle \\
 &\left. + P_{j+1}^{(1)}(\cos\theta) 2^{1/2} j (j+1)^{-1} \langle j, j+1, 1 | T | j, j+1, 1 \rangle \right\}
 \end{aligned}$$

(B6)

$$\begin{aligned}
 M_{0,0} &= (2k)^{-1} \sum_j \left\{ P_{j-1}(\cos\theta) \cdot 2j \langle j, j-1, 1 | T | j, j-1, 1 \rangle \right. \\
 &+ P_{j-1}(\cos\theta) 2 [j(j+1)]^{1/2} \langle j, j-1, 1 | T | j, j+1, 1 \rangle \\
 &+ P_{j+1}(\cos\theta) 2 [j(j+1)]^{1/2} \langle j, j+1, 1 | T | j, j-1, 1 \rangle \\
 &\left. + P_{j+1}(\cos\theta) 2(j+1) \langle j, j+1, 1 | T | j, j+1, 1 \rangle \right\}
 \end{aligned}$$

(B7)

and

$$M_{SS} = (2k)^{-1} \sum_j P_j(\cos\theta) 2(2j+1) \langle j, j, 0 | T | j, j, 0 \rangle. \quad (B8)$$

One will observe that for a given  $j$ , the only non-zero matrix elements of  $T$  are those indicated below;

$$T_j = \begin{pmatrix} T_{j,j,0} & 0 & 0 & 0 \\ 0 & T_{j-1,j-1,1} & 0 & T_{j-1,j+1,1} \\ 0 & 0 & T_{j,j,1} & 0 \\ 0 & T_{j+1,j-1,1} & 0 & T_{j+1,j+1,1} \end{pmatrix},$$

where in this 4x4 matrix we denote  $\langle j, l', s | T | j, l, s \rangle$  as  $T_{l', l, s}$ . The zeros are a consequence of spin conservation and parity conservation.

From the relativistic unitarity condition, one can show that if we denote

$$T_j = (S_j - 1)/2i \quad (B9)$$

where

$$S_j = \begin{pmatrix} S_{j,j,0} & 0 & 0 & 0 \\ 0 & S_{j-1,j-1,1} & 0 & S_{j-1,j+1,1} \\ 0 & 0 & S_{j,j,1} & 0 \\ 0 & S_{j+1,j-1,1} & 0 & S_{j+1,j+1,1} \end{pmatrix} \quad (\text{B10})$$

then

$$S_j S_j^\dagger = I_{4 \times 4} \quad (\text{B11})$$

Following established convention, e.g. ref. 14, we parameterize  $S_{j,j,0}$  and  $S_{j,j,1}$  as

$$S_{j,j,0} = \exp(2i\delta_{j,j,0})$$

and

$$S_{j,j,1} = \exp(2i\delta_{j,j,1}).$$

(B12a)

For the matrix elements  $S_{j\pm 1, j\pm 1, 1}$ , we generalize the Stapp-Ypsilantis-Metropolis (SYM) parameterization<sup>14</sup> of the time-reversal-symmetric scattering matrix, to write

$$S_{j\pm} = \begin{pmatrix} S_{j-, j-, 1} & S_{j-, j+, 1} \\ S_{j+, j-, 1} & S_{j+, j+, 1} \end{pmatrix} \quad (\text{B12b})$$

$$= e^{i\delta_j} e^{i\varepsilon_j} e^{2i\lambda_j} e^{i\tilde{\delta}_j} e^{i\tilde{\delta}_j},$$

where

$$\delta_j = \begin{pmatrix} S_{j, j-1} & 0 \\ 0 & S_{j, j+1} \end{pmatrix}$$

$$\varepsilon_j = \begin{pmatrix} 0 & \varepsilon_j \\ \varepsilon_j & 0 \end{pmatrix} = \varepsilon_j \sigma_1$$

and

$$\lambda_j = \begin{pmatrix} 0 & -i\lambda_j \\ i\lambda_j & 0 \end{pmatrix} = \lambda_j \sigma_2.$$

This parameterization satisfies the unitarity condition pertaining to the  $l=j\pm 1$  submatrix;

$$S_{j\pm} S_{j\pm}^\dagger = 1_{2 \times 2}.$$

Explicitly,

$$S_{j\pm} = \begin{pmatrix} e^{2i\delta_{j,i-1}} \cos 2\varepsilon_j \cos 2\lambda_j, & e^{i(\delta_{j,i-1} + \delta_{j,j+1})} (i \sin 2\varepsilon_j \cos 2\lambda_j + \sin 2\lambda_j) \\ e^{i(\delta_{j,i-1} + \delta_{j,i+1})} (i \sin 2\varepsilon_j \cos 2\lambda_j - \sin 2\lambda_j), & e^{2i\delta_{j,i+1}} \cos 2\varepsilon_j \cos 2\lambda_j \end{pmatrix}$$

(B13)

In a calculation of  $S_{j\pm}$  from some basic interaction, such as  $A_1$ -exchange and other boson-exchange iterated in a Blankenbecler-Sugar equation, it is convenient to compute the K-matrix rather than the T-matrix. (This is especially so when time-reversal symmetry holds, for then K has only real elements. Even when time-reversal symmetry fails, K is hermitian and easier to calculate than T.) The K-matrix is related to the S-matrix for states of total angular momentum  $j$  by

$$S_j = (1 - iK_j)^{-1} (1 + iK_j), \quad (B14)$$

where

$$K_j = \begin{pmatrix} K_{j,i,0} & 0 & 0 & 0 \\ 0 & K_{j-1,i-1,1} & 0 & K_{j-1,i+1,1} \\ 0 & 0 & K_{j,i,1} & 0 \\ 0 & K_{j+1,j-1,1} & 0 & K_{j+1,j+1,1} \end{pmatrix} \quad (B15)$$

For the uncoupled states, the conventional phase-shift parameterization of  $S_j$  (eq. B10) leads to

$$\tan \delta_{j,j,0} = K_{j,j,0}$$

and

$$\tan \delta_{j,j,1} = K_{j,j,1}$$

(B16)

For the coupled states, the relationship between the K-matrix elements and the S-matrix phase parameters is somewhat more complicated. By eq. B14

$$S_{j\pm} = A_j^{-1} \begin{pmatrix} (1 + iK_{j+1,j-1})(1 - iK_{j+1,j+1}) - K_{j+1,j+1} K_{j+1,j-1} & 2iK_{j-1,j+1} \\ 2iK_{j+1,j-1} & (1 - iK_{j-1,j-1})(1 + iK_{j+1,j+1}) - K_{j-1,j+1} K_{j+1,j-1} \end{pmatrix},$$

(B17)

where

$$A_j = 1 - K_{j+1,j-1} K_{j+1,j+1} + K_{j-1,j+1} K_{j+1,j-1} - i(K_{j-1,j-1} + K_{j+1,j+1}).$$

It is easy to relate the quantity  $(\delta_{j,j-1} - \delta_{j,j+1})$  to the K-matrix elements; we observe that from eq. B13

$$S_{j-1,j-1,1} / S_{j+1,j+1,1} = \exp 2i(\delta_{j,j-1} - \delta_{j,j+1})$$

which, by eq. B17

$$= \left[ (1 + i K_{j-1,j-1}) (1 - i K_{j+1,j+1}) - K_{j-1,j+1} K_{j+1,j-1} \right] \cdot \\ \times \left[ (1 - i K_{j-1,j-1}) (1 + i K_{j+1,j+1}) - K_{j-1,j+1} K_{j+1,j-1} \right]^{-1}$$

and since the denominator of this expression is the complex conjugate of the numerator.

$$= \exp \left\{ 2i \arg \left[ (1 + i K_{j-1,j-1}) (1 - i K_{j+1,j+1}) - K_{j-1,j+1} K_{j+1,j-1} \right] \right\}$$

Thus

$$\delta_{j,j-1} - \delta_{j,j+1} \\ = \arg \left[ (1 + i K_{j-1,j-1}) (1 - i K_{j+1,j+1}) - K_{j-1,j+1} K_{j+1,j-1} \right] \\ = \arg \left[ (1 + K_{j-1,j-1} K_{j+1,j+1} - K_{j-1,j+1} K_{j+1,j-1}) \right. \\ \left. + i (K_{j-1,j-1} - K_{j+1,j+1}) \right]. \quad (B18)$$

$\delta_{j,j-1} - \delta_{j,j+1}$  can thus be depicted as in fig. 12a. One observes from this figure that

$$\tan (\delta_{j,j-1} - \delta_{j,j+1}) = (K_{j-1,j-1} - K_{j+1,j+1}) \\ \times (1 + K_{j-1,j-1} K_{j+1,j+1} - K_{j-1,j+1} K_{j+1,j-1})^{-1}. \quad (B19)$$

Note that in the limit of a weak interaction, where the K-matrix elements approach zero, then

$$\delta_{j,j-1} - \delta_{j,j+1} = K_{j-1,j-1} - K_{j+1,j+1} \quad (B20)$$

It is similarly easy to relate the quantity  $\delta_{j,j-1} + \delta_{j,j+1}$  to the K-matrix elements. We take the  $j-1, j-1$  element of eq. B17,

$$S_{j-1,j-1} = \Delta_j^{-1} \left[ (1 + iK_{j-1,j-1})(1 - iK_{j+1,j+1}) - K_{j-1,j+1} K_{j+1,j-1} \right]$$

parameterize it using eqs. B13 and B18,

$$\begin{aligned} (\exp 2i\delta_{j,j-1}) \cos 2\varepsilon_j \cos 2\lambda_j &= \left[ \exp i(\delta_{j,j-1} - \delta_{j,j+1}) \right] \\ &\times \left| (1 + iK_{j-1,j-1})(1 - iK_{j+1,j+1}) - K_{j-1,j+1} K_{j+1,j-1} \right| \\ &/ |\Delta_j| \exp(i \arg \Delta_j) \end{aligned}$$

and thereby observe that

$$\arg \Delta_j = -(\delta_{j,j-1} + \delta_{j,j+1}) \quad (B21)$$

We therefore construct fig. 12b and write down immediately that

$$\begin{aligned} \tan(\delta_{j,j-1} + \delta_{j,j+1}) &= (K_{j-1,j-1} + K_{j+1,j+1}) \\ &\times (1 - K_{j-1,j-1} K_{j+1,j+1} + K_{j-1,j+1} K_{j+1,j-1})^{-1} \quad (B22) \end{aligned}$$

In the limit of a weak interaction,

$$\delta_{j,j-1} + \delta_{j,j+1} = K_{j-1,j-1} + K_{j+1,j+1} \quad (\text{B23})$$

Thus using this result and eq. B20, we see that in this limit,

$$\delta_{j,j-1} = K_{j-1,j-1}$$

and

$$\delta_{j,j+1} = K_{j+1,j+1} \quad (\text{B24})$$

To relate  $\epsilon_j$  to the K-matrix elements, we observe from eq. B13 that

$$(S_{j-1,j+1} + S_{j+1,j-1}) / (S_{j-1,j-1} S_{j+1,j+1})^{1/2} = 2i \tan 2\epsilon_j$$

which from eq. B17 also

$$= 2i (K_{j-1,j+1} + K_{j+1,j-1}) / \left| (1 + i K_{j-1,j-1}) (1 - i K_{j+1,j+1}) - K_{j-1,j+1} K_{j+1,j-1} \right|$$

Now,  $K_{j\pm}$  is hermitian when the interaction is hermitian, which we assume to be the case in order to conserve particle number.

Thus  $2i(K_{j-1,j+1} + K_{j+1,j-1}) = 4i \operatorname{Re} K_{j-1,j+1}$  and

$$\tan 2\varepsilon_j = 2 \operatorname{Re} K_{j-1, j+1} \times \left[ (1 + K_{j-1, j-1} K_{j+1, j+1} - K_{j-1, j+1} K_{j+1, j-1})^2 + (K_{j-1, j-1} - K_{j+1, j+1})^2 \right]^{-\frac{1}{2}}.$$

(B25)

Again we note that in the limit of very small K-matrix elements, a simple expression results;

$$\varepsilon_j = \operatorname{Re} K_{j-1, j+1}.$$

(B26)

Finally, let us relate  $\lambda_j$  to the K-matrix elements. We observe from eq. B13 that

$$S_{j-1, j+1} - S_{j+1, j-1} = 2 \sin 2\lambda_j \exp i(\delta_{j, j-1} + \delta_{j, j+1})$$

and that, from eq. B17 it also

$$= 2i (K_{j-1, j+1} - K_{j+1, j-1}) / \Delta_j$$

taking into account eq. B21 we see that it further

$$= 2i (K_{j-1, j+1} - K_{j+1, j-1}) / |\Delta_j| \exp [-i(\delta_{j, j-1} + \delta_{j, j+1})].$$

Thus the exponents cancel; the hermitricity of K yields

$$\begin{aligned}
 \sin 2\lambda_j &= (2 \operatorname{Im} K_{j+1, j-1}) / |\Delta_j| \\
 &= 2 \operatorname{Im} K_{j+1, j-1} \\
 &\quad \times \left[ (1 - K_{j-1, j-1} K_{j+1, j+1} + K_{j-1, j+1} K_{j+1, j-1})^2 \right. \\
 &\quad \left. + (K_{j-1, j+1} + K_{j+1, j-1})^2 \right]^{-\frac{1}{2}}
 \end{aligned}
 \tag{B27}$$

In the limit as the interaction vanishes,

$$\lambda_j = \operatorname{Im} K_{j+1, j-1}
 \tag{B28}$$

Phillips has suggested another parameterization of the S-matrix to take into account time-irreversibility;<sup>19)</sup> he uses the format (albeit with an opposite sign convention for  $\lambda_j$ )

$$S_{j\pm} = e^{-i\bar{\lambda}_j} \tilde{S}_{j\pm} e^{i\bar{\lambda}_j}
 \tag{B29}$$

where

$$\bar{\lambda}_j = \begin{pmatrix} \bar{\lambda}_j & 0 \\ 0 & -\bar{\lambda}_j \end{pmatrix} = \bar{\lambda}_j \sigma_3$$

and where  $\tilde{S}_{j\pm}$  is a symmetric 2x2 matrix. Phillips parameterizes  $\tilde{S}_{j\pm}$  according to the Blatt-Biedenharn (BB) convention<sup>20)</sup> but this parameterization has been nearly universally abandoned in favor of the SYM parameterization<sup>14)</sup> because the BB convention can lead to very large values for the mixing parameter for even a very weak interaction if  $(K_{j-1,j-1} - K_{j+1,j+1})$  is as small as  $K_{j-1,j+1}$ . We therefore shall also elect to parameterize  $\tilde{S}_{j\pm}$  according to the SYM convention. Even with this parameterization, however, one of Phillips' phase parameters ( $\lambda_j$ ) does not necessarily reduce to a small value in the limit of a vanishing interaction, as we will show. We set

$$\tilde{S}_{j\pm} = e^{i\bar{\delta}_j} e^{2i\bar{\epsilon}_j} e^{i\bar{\delta}_j} \quad (\text{B30})$$

where

$$\bar{\delta}_j = \begin{pmatrix} \bar{\delta}_{j,j-1} & 0 \\ 0 & \bar{\delta}_{j,j+1} \end{pmatrix}$$

and

$$\bar{\epsilon}_j = \begin{pmatrix} 0 & \bar{\epsilon}_j \\ \bar{\epsilon}_j & 0 \end{pmatrix} = \bar{\epsilon}_j \sigma_1$$

Thus

$$S_{j\pm} = e^{-i\bar{\lambda}_j \sigma_3} e^{i\bar{\delta}_j} e^{2i\bar{\epsilon}_j} e^{i\bar{\delta}_j} e^{i\bar{\lambda}_j \sigma_3}$$

$$= \begin{pmatrix} \cos 2\bar{\varepsilon}_j e^{2i\bar{\delta}_{j,j-1}} & i \sin 2\bar{\varepsilon}_j e^{i(\bar{\delta}_{j,j-1} + \bar{\delta}_{j,j+1})} e^{-2i\bar{\lambda}_j} \\ i \sin 2\bar{\varepsilon}_j e^{i(\bar{\delta}_{j,j-1} + \bar{\delta}_{j,j+1})} e^{2i\bar{\lambda}_j} & \cos 2\bar{\varepsilon}_j e^{2i\bar{\delta}_{j,j+1}} \end{pmatrix}$$

(B31)

We can relate  $\bar{\delta}_{j,j-1}$ ,  $\bar{\delta}_{j,j+1}$ ,  $\bar{\varepsilon}_j$ , and  $\bar{\lambda}_j$  to the elements of the K-matrix just as we related  $\delta_{j,j-1}$ ,  $\delta_{j,j+1}$ ,  $\varepsilon_j$ , and  $\lambda_j$  to these elements. We equate the r.h.s. of eq. B31 with the r.h.s. of eq. B17 and immediately show that  $(\bar{\delta}_{j,j-1} - \bar{\delta}_{j,j+1})$  equals the r.h.s. of eq. B18, hence equals  $(\delta_{j,j-1} - \delta_{j,j+1})$ . We show almost as easily that

$$\bar{\delta}_{j,j-1} + \bar{\delta}_{j,j+1} = -\arg \Delta_j$$

and hence

$$= \delta_{j,j-1} + \delta_{j,j+1}$$

Thus

$$\bar{\delta}_{j,j-1} = \delta_{j,j-1}$$

and

$$\bar{\delta}_{j,j+1} = \delta_{j,j+1}$$

To relate  $\epsilon_j$  to the K-matrix elements we observe that

$$\begin{aligned} & (S_{j-1,j+1} S_{j+1,j-1} / S_{j-1,j-1} S_{j+1,j+1})^{\frac{1}{2}} \\ &= i \tan 2\bar{\epsilon}_j \\ &= 2i |K_{j-1,j+1}| \\ & \quad / |(1 + i K_{j-1,j-1})(1 - i K_{j+1,j+1}) - K_{j-1,j+1} K_{j+1,j-1}| \end{aligned}$$

hence

$$\begin{aligned} \tan 2\bar{\epsilon}_j &= 2 |K_{j-1,j+1}| \\ & \quad \times \left[ (1 + K_{j-1,j-1} K_{j+1,j+1} - K_{j-1,j+1} K_{j+1,j-1})^2 \right. \\ & \quad \left. + (K_{j-1,j-1} - K_{j+1,j+1})^2 \right]^{-\frac{1}{2}} \end{aligned} \tag{B32}$$

Observe that the formula for  $\tan 2\epsilon_j$  differs from that for  $\tan 2\bar{\epsilon}_j$  only in that  $|K_{j-1,j+1}|$  replaces  $\text{Re } K_{j-1,j+1}$ .

Finally, to relate  $\lambda_j$  to the K-matrix, we note that

$$\begin{aligned} S_{j+1,j-1} / S_{j-1,j+1} &= \exp(4i \bar{\lambda}_j) \\ &= K_{j+1,j-1} / K_{j-1,j+1} \end{aligned}$$

where we have used eqs. B17 and B31. Since  $K_{j-1,j+1} = (K_{j+1,j-1})^*$ ,

$$\exp(4i\bar{\lambda}_j) = \exp(2i \arg K_{j-1,j+1})$$

or

$$\tan 2\bar{\lambda}_j = \text{Im } K_{j+1,j-1} / \text{Re } K_{j+1,j-1} \quad (\text{B33})$$

Now observe that even in the limit of a very weak interaction,  $\bar{\lambda}_j$  can approach  $45^\circ$  if  $\text{Re } K_{j+1,j-1}$  happens to be zero. This in fact happens in the BG model; as the laboratory energy increases from 0 to 500 MeV,  $\epsilon_2$  goes from  $0^\circ$  to a minimum of about  $-3^\circ$  and then back up through  $0^\circ$  to positive values at about 450 MeV.  $\text{Re } K_{j+1,j-1} = \text{Re } K_{31}$  behaves similarly to  $\epsilon_2$  (as suggested by eq. B25 or eq. B32) and so at 450 MeV,  $\text{Re } K_{31} = 0$ , so that  $\tan 2\lambda_2 = \infty$ . Thus  $\lambda_2 = 45^\circ$ , despite the fact that  $\tan K_{31}$  is very small. On the other hand,  $\lambda_2 = -0.6$  at 450 MeV, so our parameterization gives a realistic measure of the strength of the interaction.

We now give the partial-wave expansion of the invariant amplitude  $t(\theta)$  of eq. A6. We observe that

$$\text{Tr} [ M(\sigma_P^a \sigma_8^b + \sigma_8^a \sigma_P^b) ] = 8t(\theta).$$

Then since

$$\sigma_P^a \sigma_8^b + \sigma_8^a \sigma_P^b = \sin \theta \begin{pmatrix} 0 & 0 & 0 & 0 \\ 0 & -1 & 0 & 1 \\ 0 & 0 & 2 & 0 \\ 0 & 1 & 0 & -1 \end{pmatrix} + \sqrt{2} \cos \theta \begin{pmatrix} 0 & 0 & 0 & 0 \\ 0 & 0 & 1 & 0 \\ 0 & 1 & 0 & -1 \\ 0 & 0 & -1 & 0 \end{pmatrix}$$

we find that

$$t = \frac{1}{4} \left[ \sin \theta (-M_{1,1} + M_{0,0} + M_{1,-1}) + \sqrt{2} \cos \theta (M_{1,0} + M_{0,1}) \right]. \quad (\text{B34})$$

It is now a simple matter to use eqs. B3 - B7 to obtain the partial-wave T-matrix element representation of  $t(\theta)$ . The result is

$$t = (4k)^{-1} \sum_{j=1}^{\infty} (2j+1) [j(j+1)]^{-\frac{1}{2}} P_j^{(1)}(\cos \theta) \times (T_{j-1,j+1,1} - T_{j+1,j-1,1}). \quad (\text{B35})$$

In terms of the parameterization of the S-matrix given by eqs. B12 and B13,

$$t = (2k)^{-1} \sum_{j=1}^{\infty} (2j+1) [j(j+1)]^{-\frac{1}{2}} P_j^{(1)}(\cos \theta) \times e^{i(\delta_{j,j-1} + \delta_{j,j+1})} \sin 2\lambda_j. \quad (\text{B36})$$

Observe that this time-irreversible amplitude vanishes if all  $\lambda_j$  vanish, or equivalently, if the r.h.s. of eq. B34 is zero.

Appendix C. Proton-proton scattering

The formulas for the NN M-matrix developed in Appendices A and B are for dissimilar particles in the absence of a Coulomb interaction, i.e. for the np system. We now determine the formulas corresponding to the pp system. The result is similar to that given in Table III of ref. 14.

The Coulomb interaction is taken into account by replacing  $S_j$ , (eq. B10) by

$$e^{i\Phi_j} S_j^N e^{i\Phi_j} \quad (C1)$$

where

$$\Phi_j = \begin{pmatrix} \phi_j & 0 & 0 & 0 \\ 0 & \phi_{j-1} & 0 & 0 \\ 0 & 0 & \phi_j & 0 \\ 0 & 0 & 0 & \phi_{j+1} \end{pmatrix} \quad (C1a)$$

Here

$$\phi_l = \eta_l - \eta_0$$

where

$$\eta_l = \arg T(l + 1 + i\eta)$$

with

$$\underline{\eta} = m e^2 / 2 \hbar^2 k = \underline{\alpha} m c / 2 \hbar k.$$

Thus

$$\underline{\eta}_l - \underline{\eta}_0 = \sum_{m=1}^l \arctan(\underline{\eta}/m).$$

If we parameterize  $S_j$  and  $S_j^N$  according to eq. B12, then the effect of replacing  $S_j$  by  $(\exp i\phi_j)S_j^N \exp i\phi_j$  is that

$$\begin{aligned} \epsilon_j &\rightarrow \epsilon_j^N, \\ \lambda_j &\rightarrow \lambda_j^N, \\ \delta_{j,j,0} &\rightarrow \delta_{j,j,0}^N + \phi_j, \\ \delta_{j,j,1} &\rightarrow \delta_{j,j,1}^N + \phi_j, \\ \delta_{j,j-1} &\rightarrow \delta_{j,j-1}^N + \phi_{j-1}, \end{aligned} \tag{C2}$$

and

$$\delta_{j,j+1} \rightarrow \delta_{j,j+1}^N + \phi_{j+1}$$

the  $\delta_{j|s}^N$  are so-called "nuclear" phase shifts and differ (usually slightly) from the purely hadronic phase shifts  $\delta_{j|s}$ .  $\epsilon_j^N$  and  $\lambda_j^N$  likewise differ slightly from  $\epsilon_j$  and  $\lambda_j$ . The simplicity of the last two substitutions is a result of the way we choose to parameterize  $S_{j\pm}$ . The Phillips parameterization does not lead to such a simple modification.

If the substitutions given in (C2) are made in the formulas for the M-matrix elements  $M_{SS}$  and  $M_{m_S m_S'}$  (eqs. B3 - B8) and the summations are

carried out, then

$$\begin{aligned}
 M_{1,1}(\theta) &\rightarrow f_c(\theta) + \bar{M}_{1,1}(\theta), \\
 M_{1,0}(\theta) &\rightarrow \bar{M}_{1,0}(\theta), \\
 M_{1,-1}(\theta) &\rightarrow \bar{M}_{1,-1}(\theta), \\
 M_{0,1}(\theta) &\rightarrow \bar{M}_{0,1}(\theta), \\
 M_{0,0}(\theta) &\rightarrow f_c(\theta) + \bar{M}_{0,0}(\theta),
 \end{aligned}
 \tag{C3}$$

and

$$M_{SS}(\theta) \rightarrow f_c(\theta) + \bar{M}_{SS}(\theta).$$

Here  $f_c(\theta)$  is obtained from the partial-wave summation given in ref. 21; apart from an ignorable  $\delta$ -function at  $\cos\theta = 1$ ,

$$\begin{aligned}
 f_c(\theta) &= (2ik)^{-1} \sum_{l=0}^{\infty} (2l+1) [(\exp 2i\phi_l) - 1] P_l(\cos\theta) \\
 &= \left[ -\eta / 2k (\sin \theta/2)^2 \right] \exp \left[ -i\eta \ln (\sin \theta/2)^2 \right].
 \end{aligned}
 \tag{C3a}$$

The  $M_{msm_s}$  and  $M_{SS}$  are obtained by making the following substitutions in

the T-matrix elements in the expansions of  $M_{m_S m_S}$  and  $M_{SS}$ :

$$T_{j,j,0} = (e^{2i\delta_{j,j,0}} - 1)/2i \rightarrow e^{2i\phi_j} (e^{2i\delta_{j,j,0}^N} - 1)/2i,$$

$$T_{j,j,1} = (e^{2i\delta_{j,j,1}} - 1)/2i \rightarrow e^{2i\phi_j} (e^{2i\delta_{j,j,1}^N} - 1)/2i,$$

$$\begin{aligned} T_{j-1,j-1} &= (e^{2i\delta_{j,j-1}} \cos 2\varepsilon_j \cos 2\lambda_j - 1)/2i \\ &\rightarrow e^{2i\phi_{j-1}} (e^{2i\delta_{j,j-1}^N} \cos 2\varepsilon_j^N \cos 2\lambda_j^N - 1)/2i \end{aligned}$$

$$\begin{aligned} T_{j\mp 1, j\pm 1} &= e^{i(\delta_{j,j-1} + \delta_{j,j+1})} (i \sin 2\varepsilon_j \cos 2\lambda_j \pm \sin 2\lambda_j) \\ &\rightarrow e^{i(\delta_{j,j-1}^N + \phi_{j-1} + \delta_{j,j+1}^N + \phi_{j+1})} \\ &\quad \times (i \sin 2\varepsilon_j^N \cos 2\lambda_j^N \pm \sin 2\lambda_j^N) \end{aligned}$$

and

$$\begin{aligned} T_{j+1, j+1} &= (e^{2i\delta_{j,j+1}} \cos 2\varepsilon_j \cos 2\lambda_j - 1)/2i \\ &\rightarrow e^{2i\phi_{j+1}} (e^{2i\delta_{j,j+1}^N} \cos 2\varepsilon_j^N \cos 2\lambda_j^N - 1). \end{aligned}$$

(C4)

Bystricky, Gersten, Junod, and Lehar<sup>22)</sup> give relativistic expressions for the Coulomb contributions in eq. C3; however our nonrelativistic corrections are quite sufficient for the purpose of this paper, as the Coulomb corrections to the predictions for P-A and P<sub>A</sub>-P<sub>B</sub> are very small, indeed almost indistinguishable in the plots at the higher energies. We do of course compute k relativistically;  $k = (mc^2 T_{lab}/2)^{1/2}$ .

We next consider the corrections to the M-matrix to be made because of the indistinguishability of the protons. If

$$\chi_{\pi_f}^{a\dagger} \chi_{\nu_f}^{b\dagger} M(\tilde{k}_f, \tilde{k}_i) \chi_{\pi_i}^a \chi_{\nu_i}^b \equiv M(\tilde{k}_f, \tilde{k}_i)_{\pi_f, \nu_f, \pi_i, \nu_i}$$

is the np amplitude, as depicted in fig. 11a, then the corresponding pp amplitude is obtained by the substitution

$$M(\tilde{k}_f, \tilde{k}_i)_{\pi_f, \nu_f, \pi_i, \nu_i} \rightarrow$$

$$M(\tilde{k}_f, \tilde{k}_i)_{\pi_f, \nu_f, \pi_i, \nu_i} - M(-\tilde{k}_f, \tilde{k}_i)_{\nu_f, \pi_f, \pi_i, \nu_i}$$

In terms of the  $M_{s', m'_s; s m_s}$  matrix elements, this corresponds to

$$M(\theta, \phi)_{l, m'_s; l, m_s} \rightarrow M(\theta, \phi)_{l, m'_s; l, m_s}$$

$$- M(\pi - \theta, \phi + \pi)_{l, m'_s; l, m_s}$$

and

$$M(\theta, \phi)_{0,0;0,0} \rightarrow M(\theta, \phi)_{0,0;0,0} + M(\pi-\theta, \phi+\pi)_{0,0;0,0},$$

where the  $-(+)$  sign on the r.h.s. results from the symmetry (antisymmetry) of the  $S=1$  ( $0$ ) spin wave function.

If we now take into account the Coulomb interaction as well as particle identity to arrive at the pp amplitudes, we must make the following substitutions:

$$M_{1,1}(\theta, \phi) \rightarrow \bar{M}_{1,1}(\theta, \phi) + f_c(\theta) - \bar{M}_{1,1}(\pi-\theta, \phi+\pi) + f_c(\pi-\theta),$$

$$M_{1,0}(\theta, \phi) \rightarrow \bar{M}_{1,0}(\theta, \phi) - \bar{M}_{1,0}(\pi-\theta, \phi+\pi),$$

$$M_{1,-1}(\theta, \phi) \rightarrow \bar{M}_{1,-1}(\theta, \phi) - \bar{M}_{1,-1}(\pi-\theta, \phi+\pi),$$

$$M_{0,1}(\theta, \phi) \rightarrow \bar{M}_{0,1}(\theta, \phi) - \bar{M}_{0,1}(\pi-\theta, \phi+\pi),$$

$$M_{0,0}(\theta, \phi) \rightarrow \bar{M}_{0,0}(\theta, \phi) + f_c(\theta) - \bar{M}_{0,0}(\pi-\theta, \phi+\pi) + f_c(\pi-\theta),$$

and

(C5)

$$M_{ss}(\theta, \phi) \rightarrow \bar{M}_{ss}(\theta, \phi) + f_c(\theta) + \bar{M}_{ss}(\pi-\theta, \phi+\pi) + f_c(\pi-\theta).$$

The spin-triplet sums  $[\bar{M}'_{m'_s, m_s}(\theta, \phi) - \bar{M}'_{m'_s, m_s}(\pi-\theta, \phi+\pi)]$  are easily

obtained from the r.h.s. of eqs. B3 - B7 by making the Coulomb T-matrix element substitutions (eq. C4), multiplying the r.h.s. by an overall factor of 2, and summing over  $P_\ell(\cos \theta)$ ,  $P_\ell^{(1)}(\cos \theta)$ , or  $P_\ell^{(2)}(\cos \theta)$  for  $\ell =$  odd integers only. The spin-singlet sum  $[\bar{M}_{SS}(\theta, \phi) + \bar{M}_{SS}(\pi - \theta, \phi + \pi)]$  is obtained from the r.h.s. of eq. B8 by making the Coulomb T-matrix substitution (eq. C4), multiplying the r.h.s. by a factor of 2, and summing over even-integer values of  $j$  only. The resulting M-matrix elements so obtained agree with those given in Table III of ref. 14 except that  $\langle j, j-1, 1 | T | j, j+1, 1 \rangle$  is no longer equal to  $\langle j, j+1, 1 | T | j, j-1, 1 \rangle$  because of time-irreversibility.

The pp version of the time-irreversible amplitude  $t(\theta)$  can be obtained by the substitutions  $\delta_{j, j-1} \rightarrow \delta_{j, j-1}^N + \phi_{j-1}$  and  $\delta_{j, j+1} \rightarrow \delta_{j, j+1}^N + \phi_j$  and antisymmetrizing the amplitude. The result is that

$$t(\theta) \rightarrow t_{pp}(\theta) = k^{-1} \sum_{j \text{ even}} (2j+1) [j(j+1)]^{-1/2} P_j^{(1)}(\cos \theta) \times \left[ \exp i (\delta_{j, j-1}^N + \phi_{j-1} + \delta_{j, j+1}^N + \phi_j) \right] \sin 2\lambda_j.$$

(C6)

Appendix D. Derivation of  $P_A - P_B$ .

Experiment A. Fig. 4A. Let  $\hat{e}_{\sim i}$  and  $\hat{e}_{\sim f}$  be unit vectors in the direction of the initial polarization and vector  $\underline{A}$ , respectively. It is convenient to express  $\hat{e}_{\sim i}$  and  $\hat{e}_{\sim f}$  in terms of the unit vectors  $\hat{p}$  and  $\hat{q}$ .

Accordingly

$$\hat{e}_{\sim i} = \hat{e}_{\sim p} \cos(\chi_i - \theta/2) + \hat{e}_{\sim q} \sin(\chi_i - \theta/2)$$

and

$$\hat{e}_{\sim f} = \hat{e}_{\sim p} \cos(\chi_f + \theta/2) + \hat{e}_{\sim q} \sin(\chi_f + \theta/2)$$

For an initial beam of particles "a" 100% polarized in the direction  $\hat{e}_{\sim i}$  scattering off an unpolarized target, the expectation value of the spin of the scattered beam in the direction  $\hat{e}_{\sim f}$  is given by

$$P_A I_0 = \frac{1}{4} \text{Tr} (M^\dagger \underline{\sigma}^a \cdot \hat{e}_{\sim f} M \underline{\sigma}^a \cdot \hat{e}_{\sim i})$$

when parity is good.<sup>23)</sup> Here  $P_A$  is the polarization component and  $I_0$  is the unpolarized differential cross section. Since

$$\underline{\sigma}^a \cdot \hat{e}_{\sim i} = \sigma_p^a \cos \chi_i' + \sigma_q^a \sin \chi_i'$$

and

$$\underline{\sigma}^a \cdot \hat{e}_{\sim f} = \sigma_p^a \cos \chi_f' + \sigma_q^a \sin \chi_f'$$

where

$$\chi'_i = \chi_i - \theta/2$$

and

$$\chi'_f = \chi_f + \theta/2,$$

$$\begin{aligned} P_A I_0 &= \frac{1}{4} \text{Tr} (M^\dagger \sigma_p^a M \sigma_p^a) \cos \chi'_f \cos \chi'_i \\ &+ \frac{1}{4} \text{Tr} (M^\dagger \sigma_p^a M \sigma_b^a) \cos \chi'_f \sin \chi'_i \\ &+ \frac{1}{4} \text{Tr} (M^\dagger \sigma_b^a M \sigma_p^a) \sin \chi'_f \cos \chi'_i \\ &+ \frac{1}{4} \text{Tr} (M^\dagger \sigma_b^a M \sigma_b^a) \sin \chi'_f \sin \chi'_i. \end{aligned}$$

Experiment B. Fig. 4B'. This time the initial polarization is in the direction  $\hat{e}'_i$  and the final component taken along direction  $\hat{e}'_f$ , where

$$\hat{e}'_i = \hat{e}_p \cos \chi'_f - \hat{e}_b \sin \chi'_f$$

and

$$\hat{e}'_f = \hat{e}_p \cos \chi'_i - \hat{e}_b \sin \chi'_i.$$

Thus

$$\begin{aligned}
 P_B I_0 &= \frac{1}{4} \text{Tr} (M^\dagger \sigma^a \cdot \hat{e}'_f M \sigma^a \cdot \hat{e}'_i) \\
 &= \frac{1}{4} \text{Tr} (M^\dagger \sigma_P^a M \sigma_P^a) \cos \chi'_i \cos \chi'_f \\
 &\quad - \frac{1}{4} \text{Tr} (M^\dagger \sigma_P^a M \sigma_8^a) \cos \chi'_i \sin \chi'_f \\
 &\quad - \frac{1}{4} \text{Tr} (M^\dagger \sigma_8^a M \sigma_P^a) \sin \chi'_i \cos \chi'_f \\
 &\quad + \frac{1}{4} \text{Tr} (M^\dagger \sigma_8^a M \sigma_8^a) \sin \chi'_i \sin \chi'_f.
 \end{aligned}$$

Therefore

$$\begin{aligned}
 (P_A - P_B) I_0 &= \sin (\chi'_i + \chi'_f) \\
 &\quad \times \left( \frac{1}{4} \text{Tr} M^\dagger \sigma_P^a M \sigma_8^a \right. \\
 &\quad \left. + \frac{1}{4} \text{Tr} M \sigma_8^a M \sigma_P^a \right).
 \end{aligned}$$

Using the form of M dictated by rotational and space-inversion invariance and by isospin invariance, eq. 2-4, one evaluates the traces using the rules

$$\sigma_P^a \sigma_8^a = i \sigma_n^a \quad (P, q, n \text{ cyclic}).$$

and

$$\text{Tr } 1 = 4$$

to obtain

$$(P_A - P_B) I_0 = [\sin(x_i + x_f)] \delta \text{Re } g^{*t}.$$

We note that  $x_i + x_f = x'_i + x'_f$ .

In relating the polarization directions in the center-of-mass system to the corresponding directions in the laboratory system, Wigner rotation must be taken into account. If the transformation from the cm system to the lab system does not involve a change in direction of the momentum of the particle, then the spin does not rotate. Such a case is the transformation of the initial beam momentum from the cm to the lab system, as depicted in figs. 4A and 13a respectively. The initial polarization direction  $\hat{e}_i$  remains at an angle  $x_i$  to the beam momentum direction  $\underline{k}_i$  in either system. However in the case of the polarization of the scattered beam, the direction  $\hat{e}_f$ , which includes the angle  $x_f$  with the c-m beam direction  $\underline{k}_f$ , appears to rotate toward  $\underline{k}_{fl}$  through an angle  $\epsilon$  (the spherical defect);  $\underline{k}_{fl}$  is the direction of the scattered beam in the lab system. This rotation is illustrated in figs. 4A and 13a. In detail, the spherical defect

$$\epsilon = \theta - 2\theta_l$$

where  $\theta$  and  $\theta_l$  are the c-m and laboratory scattering angles, respectively. (This rule is derived, e.g., by Sard<sup>24</sup>).  $\theta$  and  $\theta_l$  are related by

$$\tan \theta_l = [2/(\gamma+1)]^{1/2} \tan(\theta/2)$$

where  $\gamma = (1-\beta^2)^{-1/2}$  and  $\beta c$  is the laboratory velocity of the projectiles.

The angle  $\chi_{fl}$  included between the (rotated) polarization vector  $\hat{e}_{fl}$  and the scattered beam's laboratory direction  $\hat{k}_{fl}$ , is thus related to  $\chi_f$  as follows (see fig. 13b);

$$\begin{aligned} \chi_{fl} &= \chi_f - \varepsilon + (\theta - \theta_l) \\ &= \chi_f + \theta_{lab} \end{aligned}$$

(Observe that in the extreme relativistic case as  $\gamma \rightarrow \infty$ ,  $\chi_{fl} = \chi_f$ . In this case, a pure helicity state remains a pure helicity state in both the c-m and lab systems.)

The same spin-rotation rules applied to experiment B, depicted in figs. 4B and 14a, show that the initial spin direction  $\hat{e}'_i$  does not rotate in transforming to the lab frame, while spin direction  $\hat{e}'_f$  rotates through  $\varepsilon$  into  $\hat{e}'_{fl}$ . The angle  $\chi_{il}$  included between  $\hat{e}'_{fl}$  and  $\hat{k}_{fl}$  is given in this instance by

$$\begin{aligned} \chi_{il} &= \chi_i + \varepsilon - (\theta - \theta_l) \\ &= \chi_i - \theta_l \end{aligned}$$

Footnotes

- §1. Note that in general the polarization of the scattered beam does not point along axis  $\underline{A}$ , but rather points out of the scattering plane into an arbitrary direction.
- §2. In the case of np scattering, the isospin-breaking, T-violating amplitude  $u(\theta)$  (eq. 2-3) also contributes to  $P - Q$  and  $P_A - P_B$ . Thus the angular distributions for  $P - Q$  and  $P_A - P_B$  will not remain the same for different T-asymmetric models unless these models conserve isospin. Of course, in pp scattering isospin is necessarily conserved.
- §3. This has been stressed by Simonius<sup>18)</sup>.
- §4. Since the charge-triplet  $A_1$  meson is the origin of T-violation in the BG model, the NN Born term is multiplied by an isospin factor  $\tau^a \cdot \tau^b$  which equals -3 (+1) in I=0 (1) states. This enhances the I=0 phase parameter  $\lambda_1$  over the I=1 parameter  $\lambda_2$ , but cannot account for the factor of 10 or more difference between these phase parameters.

References

- 1) E. C. G. Sudarshan, Proc. Roy. Soc. A305 (1968) 319
- 2) R. A. Bryan and A. Gersten, Phys. Rev. Letters 26 (1971) 1000, erratum 27 (1971) 1102
- 3) R. A. Bryan, Phys. Rev. C 12 (1975) 1968
- 4) W. G. Weitkamp, D. W. Storm, D. C. Shreve, W. J. Braithwaite, and D. Bodansky, Phys. Rev. 165 (1968) 1233
- 5) R. A. Bryan, Phys. Rev. D 10 (1974) 3854
- 6) R. Zulkarneev, Kh. Murtazaev, and B. Khachaturov, JINR preprint E1-9386, Dubna, 1975
- 7) R. A. Bryan and A. Gersten, Interaction Studies in Nuclei, eds. H. Jochim and B. Ziegler (North-Holland Publishing Co., Amsterdam, 1975) p. 233
- 8) A. Richter, Interaction Studies in Nuclei, eds. H. Jochim and B. Ziegler (North-Holland Publishing Co., The Netherlands, 1975) p. 191
- 9) W. B. Dress, P. D. Miller, J. M. Pendlebury, Paul Perrin, and N. F. Ramsey, Phys. Rev. D 15 (1977) 9
- 10) J. Binstock, R. Bryan, and A. Gersten, Phys. Letters 48B (1974) 77
- 11) M. H. MacGregor, M. J. Moravcsik, and H. P. Stapp, Ann. Rev. Nucl. Sci. 10 (1960) 291
- 12) L. Wolfenstein and J. Ashkin, Phys. Rev. 85 (1952) 947
- 13) R. Handler, S. C. Wright, L. Pondrom, P. Limon, S. Olsen, and P. Kloeppel, Phys. Rev. Letters 19 (1970) 933

- 14) H. P. Stapp, T. J. Ypsilantis, and N. Metropolis, Phys. Rev. 105, (1957) 302
- 15) M. H. MacGregor, R. A. Arndt, and R. M. Wright, Phys. Rev. 182 (1969) 1714
- 16) M. H. MacGregor, M. J. Moravcsik, and H. P. Stapp, Ann. Rev. Nucl. Sci. 10 (1960) 291
- 17) N. Hoshizaki, Suppl. of the Prog. of Theoret. Phys. 42 (1968) 107
- 18) M. Simonius, Phys. Letters 58B (1975) 147
- 19) R. J. N. Phillips, Nuovo cimento 8 (1958) 265
- 20) J. M. Blatt and L. C. Biedenharn, Phys. Rev. 86 (1952) 399
- 21) L. I. Schiff, Quantum Mechanics, Third Ed., (McGraw-Hill Book Co., 1968) p. 138
- 22) J. Bystricky, A. Gersten, A. Junod, and F. Lehar, CERN preprint, July 1976
- 23) L. Wolfenstein, Ann. Rev. Nucl. Sci. 6 (1956) 43
- 24) R. D. Sard, Relativistic Mechanics, (W. A. Benjamin, New York, 1970)

FIGURE CAPTIONS

- Fig. 1. Feynman diagram for the exchange of an  $A_1$ -meson between two nucleons.
- Fig. 2. Comparison of predictions for  $P - Q$  and  $P_A - P_B$  by the one-boson-exchange (BG) potential model and the "zero-range" model, for pp and np scattering, at 425 MeV. Note that the scales for all zero-range model predictions are in arbitrary units.
- Fig. 3. Experiments to measure polarization  $P$  (drawing A) and asymmetry  $Q$  (drawing B).
- Fig. 4. Measurement of  $P_A$  (drawing A) and  $P_B$  (drawing B). Drawing B' depicts experiment B rotated so that the initial and final beam momenta are parallel to those of A. All drawings for center-of-mass system.
- Fig. 5. Possible transitions between angular momentum states in np and pp scattering when the interaction is invariant under rotations and inversions in ordinary space ( $j$  and  $P$  conserved, respectively) and when it is invariant under rotations in isospin space ( $I$  good).
- Fig. 6. The time-irreversible phase parameter  $\lambda_j$  predicted by the BG model for  $j=1$  through 4, for  $0 \leq T_{lab} \leq 635$  MeV.

Fig. 7. Predictions of the zero-range model for  $(P - \mathcal{Q})/\lambda_2$  and  $(P_A - P_B)/\lambda_2$  in pp scattering, with  $\lambda_2$  measured in radians.

Fig. 8. Predictions of the zero-range model for  $(P - \mathcal{Q})/\lambda_1$  and  $(P_A - P_B)/\lambda_1$  in np scattering, with  $\lambda_1$  in radians.

Fig. 9. Predictions of the BG model for  $P - \mathcal{Q}$  and  $P_A - P_B$  in pp scattering; the solid (dashed) curves correspond to choosing  $F_A = g_A(-g_A)$  in the Sudarshan model (see text preceding eq. 1-2).

Fig. 10. Predictions of the BG model for  $P - \mathcal{Q}$  and  $P_A - P_B$  in np scattering; solid (dashed) curves as defined in caption of fig. 9.

Fig. 11. Scattering of fermion "a" off fermion "b" in the center-of-mass system. (a) initial and final spins of a are denoted  $\pi_i$  and  $\pi_f$ ; of b denoted  $\nu_i$  and  $\nu_f$ . Initial and final momenta as indicated. (b) Space-inverted spins and momenta; initial and final spins of a are denoted  $\underline{\pi}_i$  and  $\underline{\pi}_f$ ; of b denoted  $\underline{\nu}_i$  and  $\underline{\nu}_f$ . Momenta (underlined) as indicated. (c) Time-reversed spins and momenta; initial and final spins of a denoted  $\bar{\pi}_i$  and  $\bar{\pi}_f$ , of b denoted  $\bar{\nu}_i$  and  $\bar{\nu}_f$ . Momenta (underlined) as indicated.

Fig. 12. Geometrical relationships between the NN phase parameters  $\delta_{j,j-1}$  and  $\delta_{j,j+1}$ , and elements of the K-matrix.

Fig. 13. (a) Part A of the  $P_A - P_B$  experiment depicted for the laboratory system. (b) Relationship of Wigner rotation angle  $\epsilon$  and the center-of-mass and laboratory scattering angles  $\theta$  and  $\theta_\ell$ .

Fig. 14. (a) Part B of the  $P_A - P_B$  experiment shown in the lab system. (b) Relationship of Wigner rotation angle  $\epsilon$  and the c-m and lab scattering angles  $\theta$  and  $\theta_\ell$ .

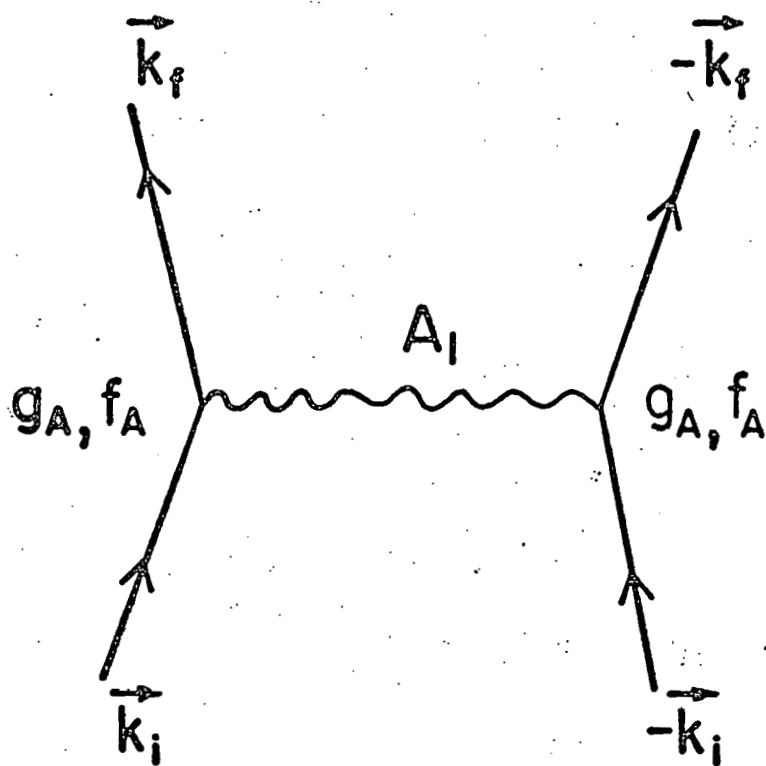
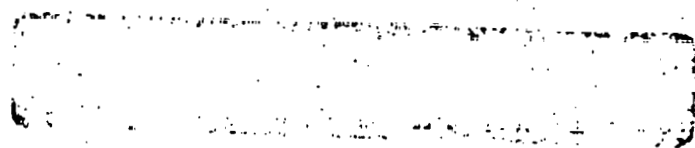
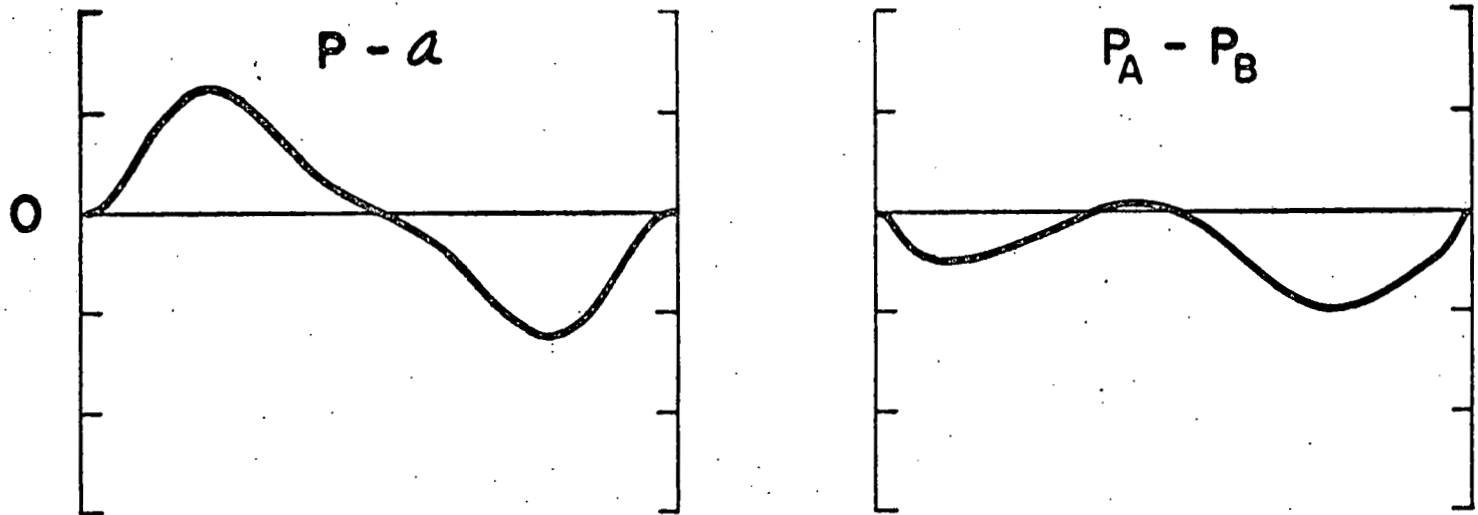


Fig. 1



p-p OBSERVABLES at 425 MeV

ZERO-RANGE MODEL



POLYNOMIAL BG MODEL

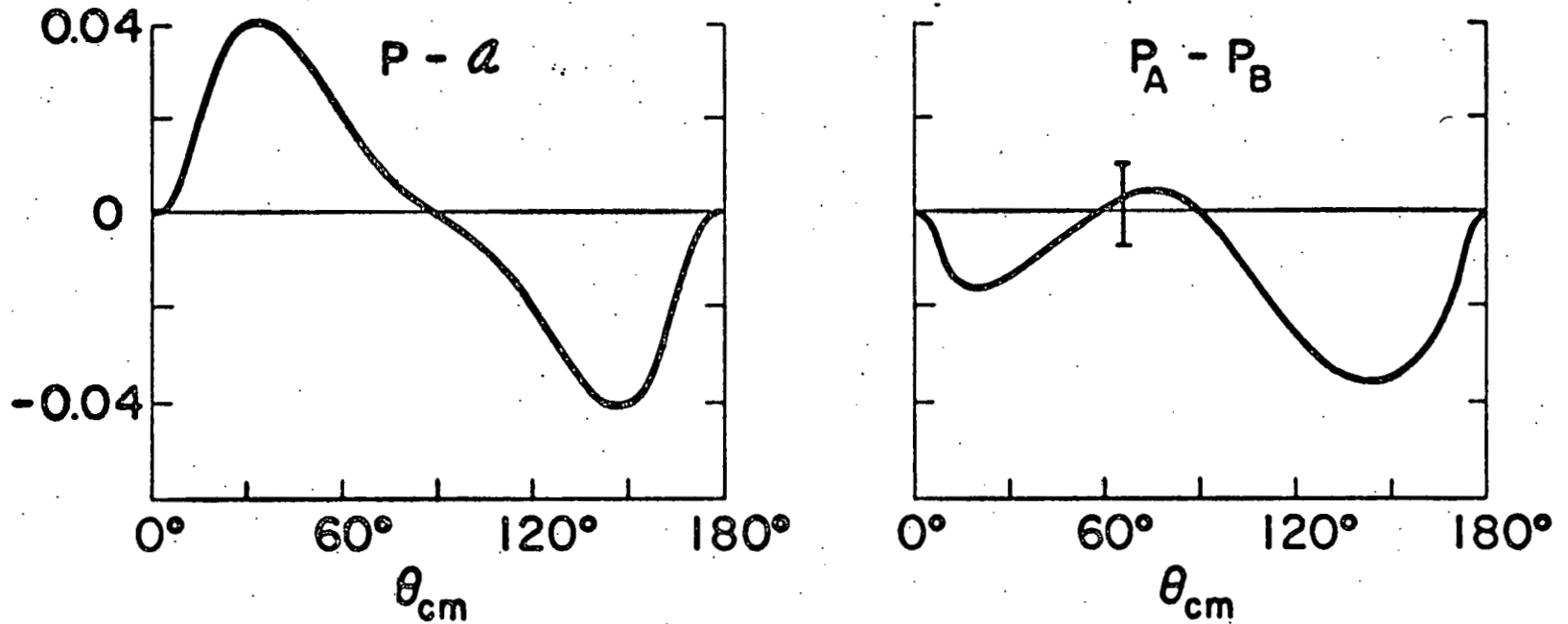
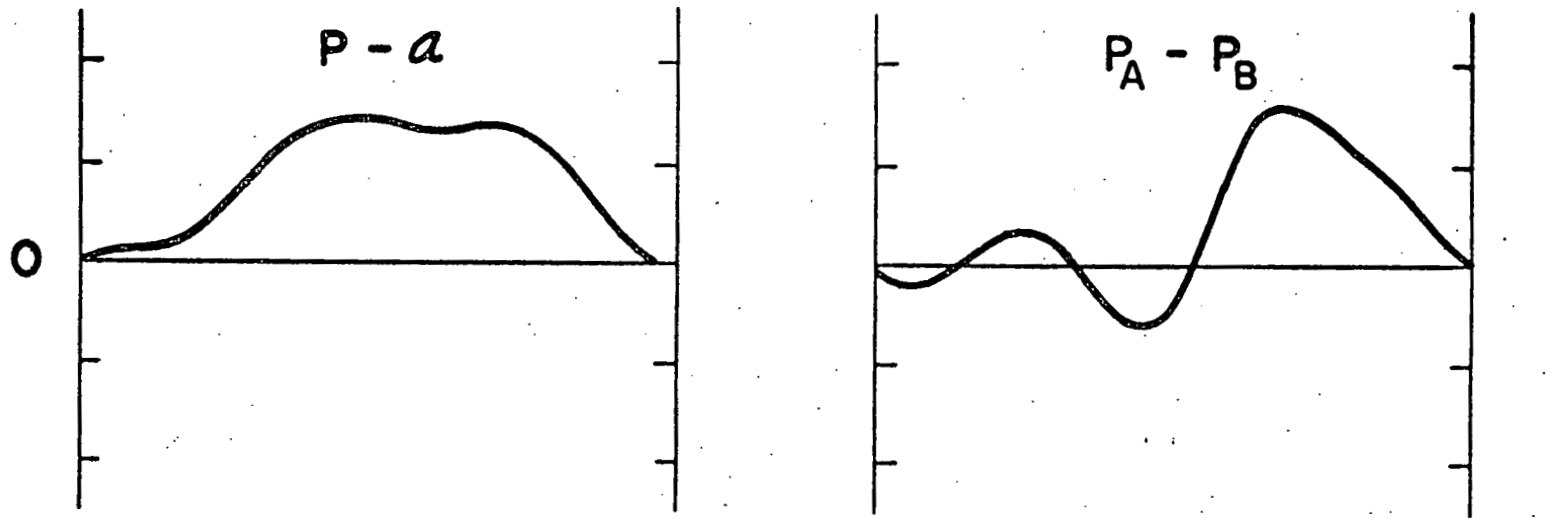


fig. 2a

n - p OBSERVABLES at 425 MeV

ZERO-RANGE MODEL



BG MODEL

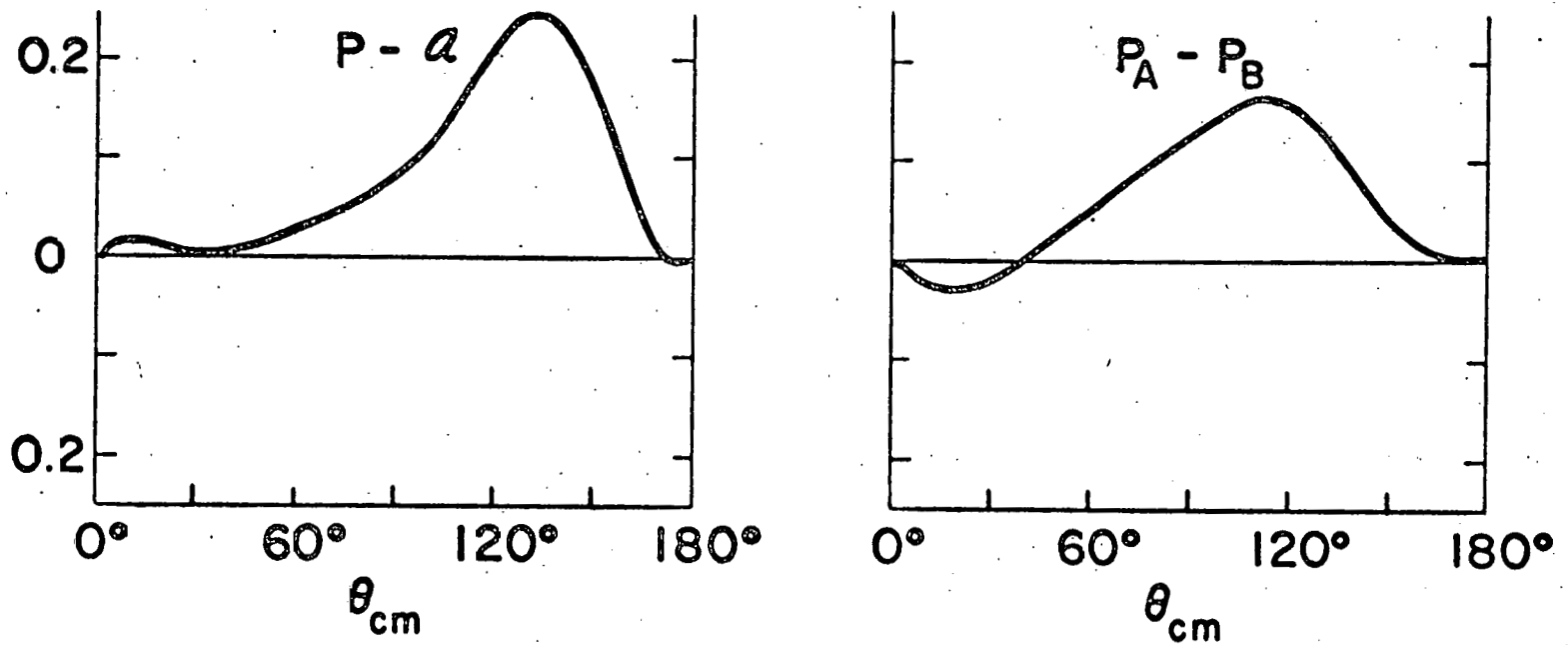
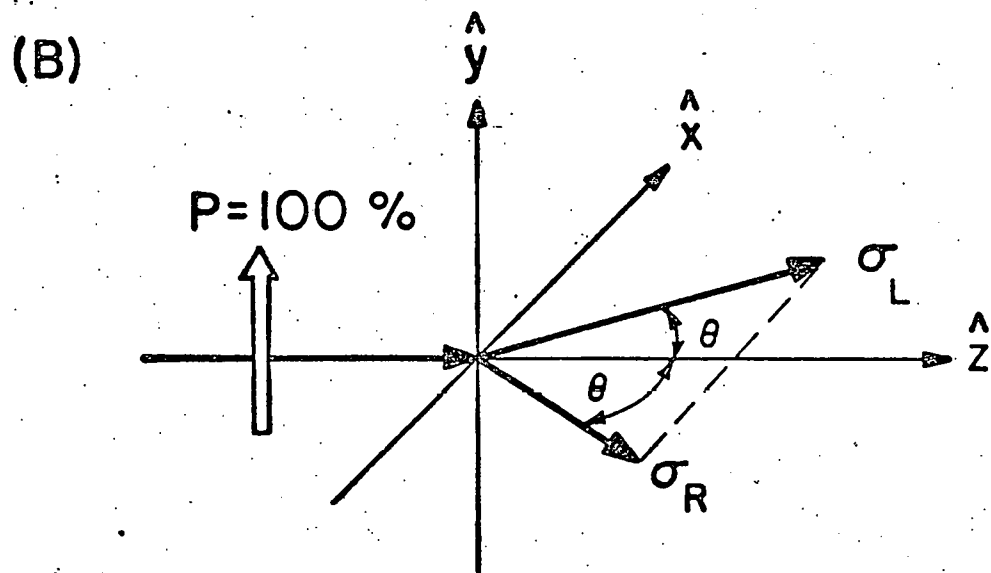
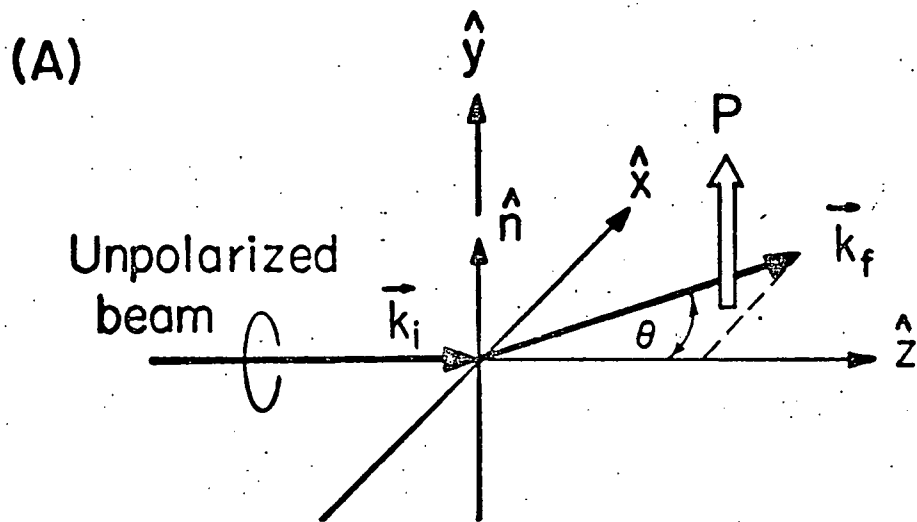


fig. 2b



XBL716-3715

fig. 3



np states

pp states

j, P good

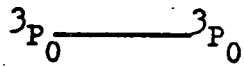
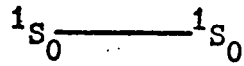
j, P, I good

j, P good

j = 0 states

j = 0 states

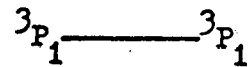
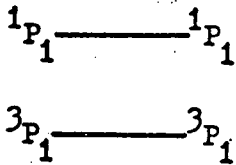
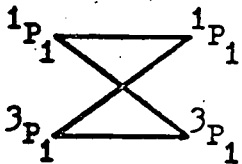
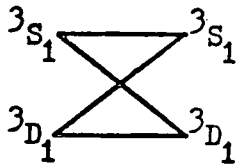
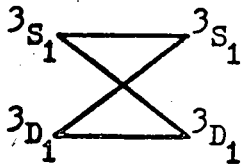
j = 0 states



j = 1 states

j = 1 states

j = 1 state



j = 2 states

j = 2 states

j = 2 states

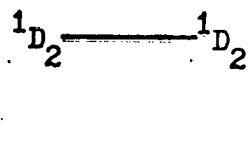
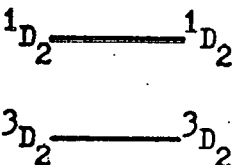
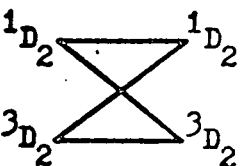
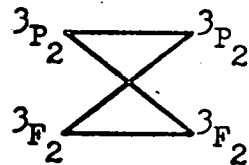
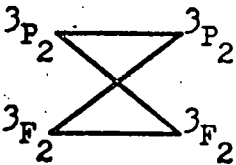
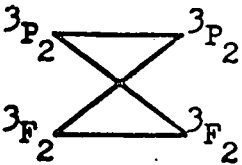


fig. 5

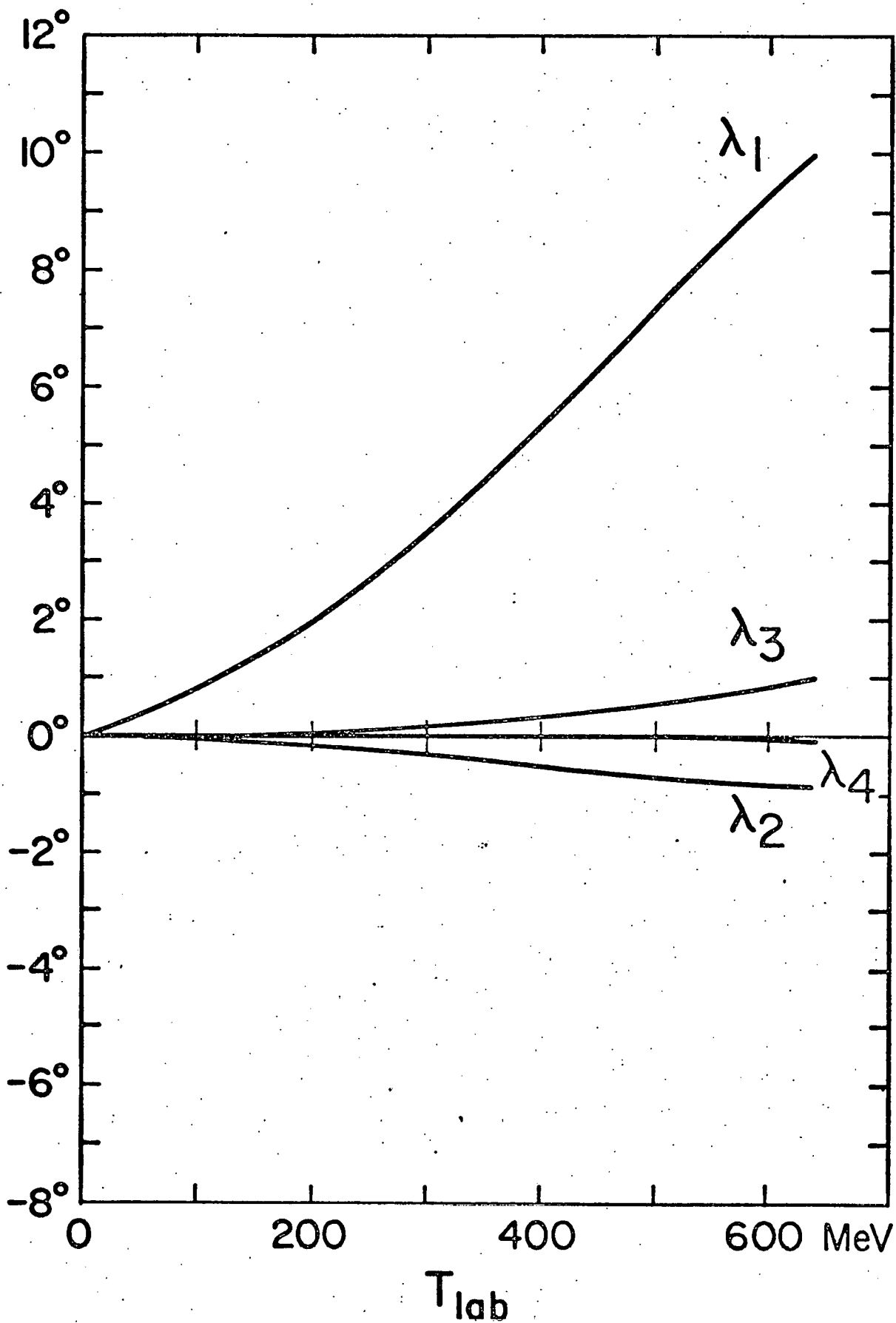
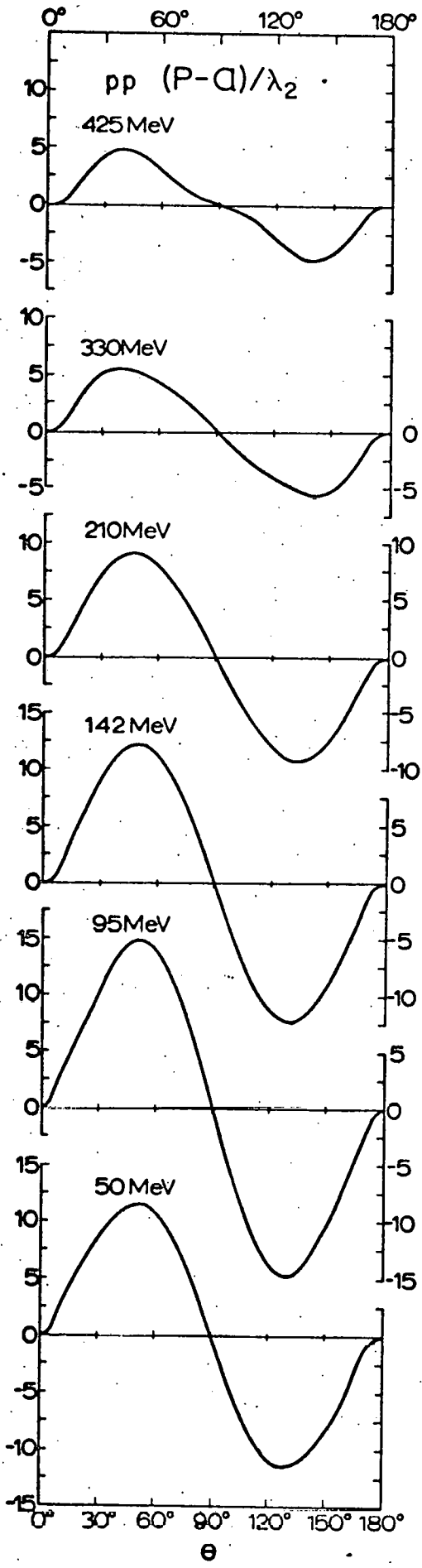


fig. 6



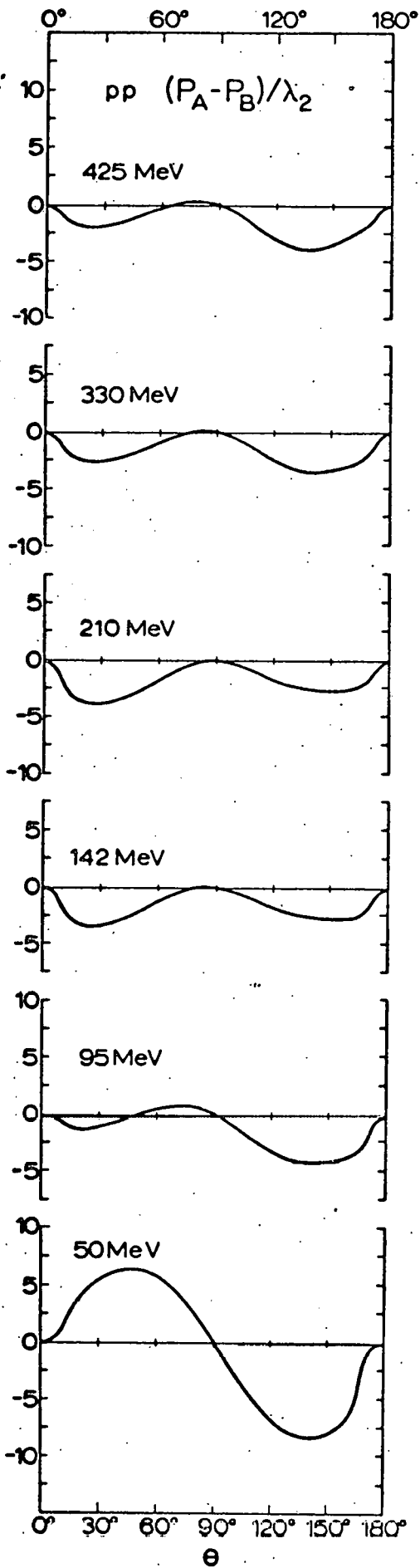
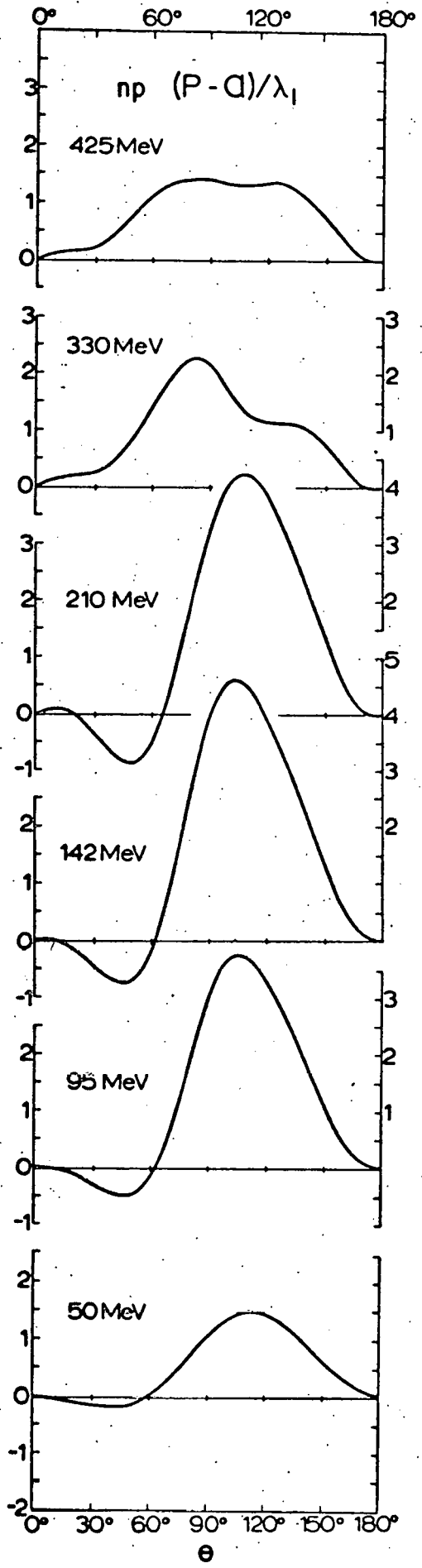


fig. 7a

fig. 7b



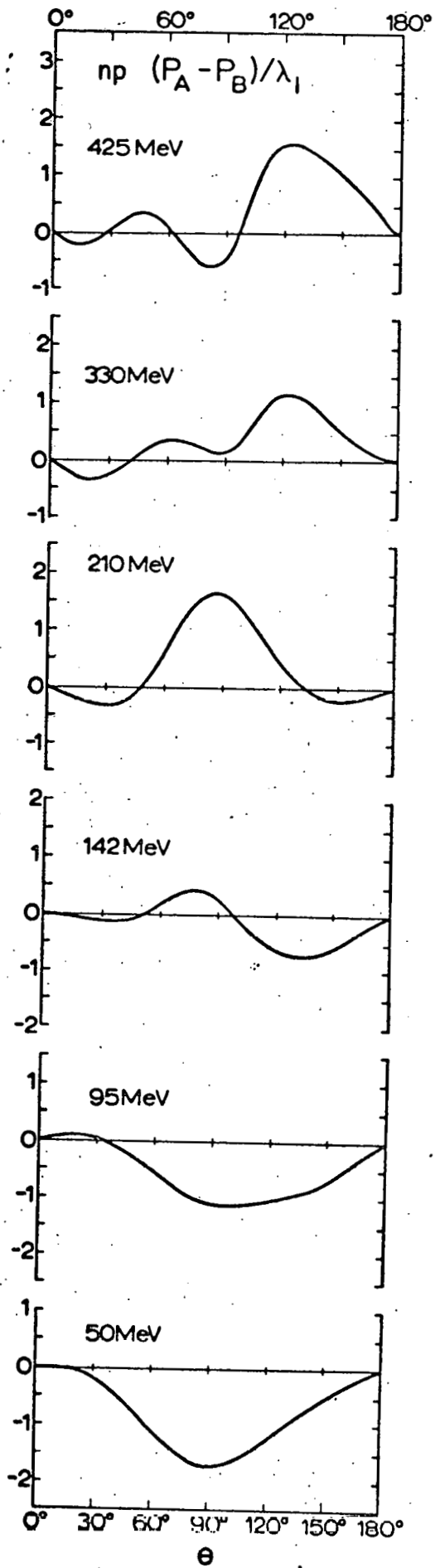


fig. 8a

fig. 8b

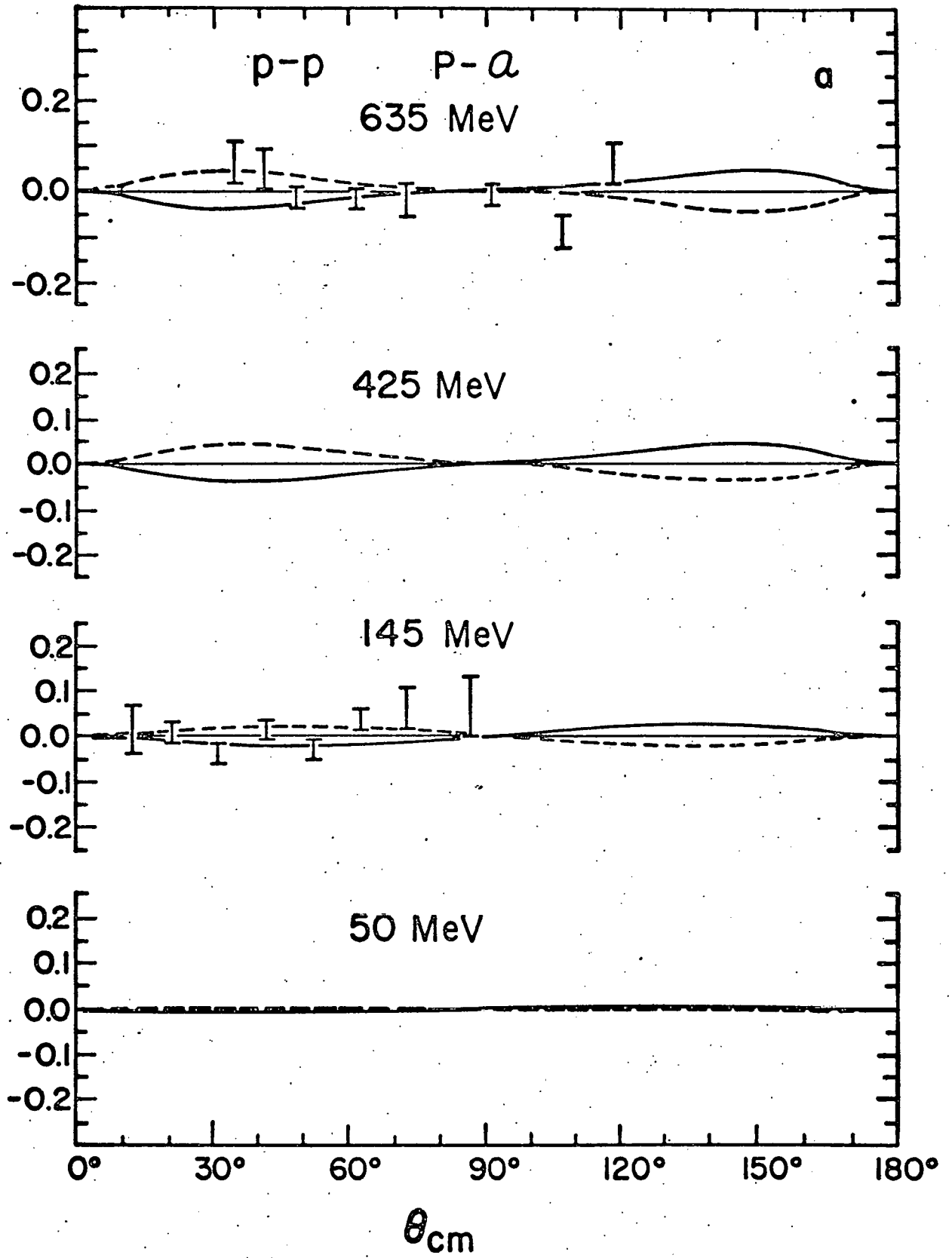


fig. 9a

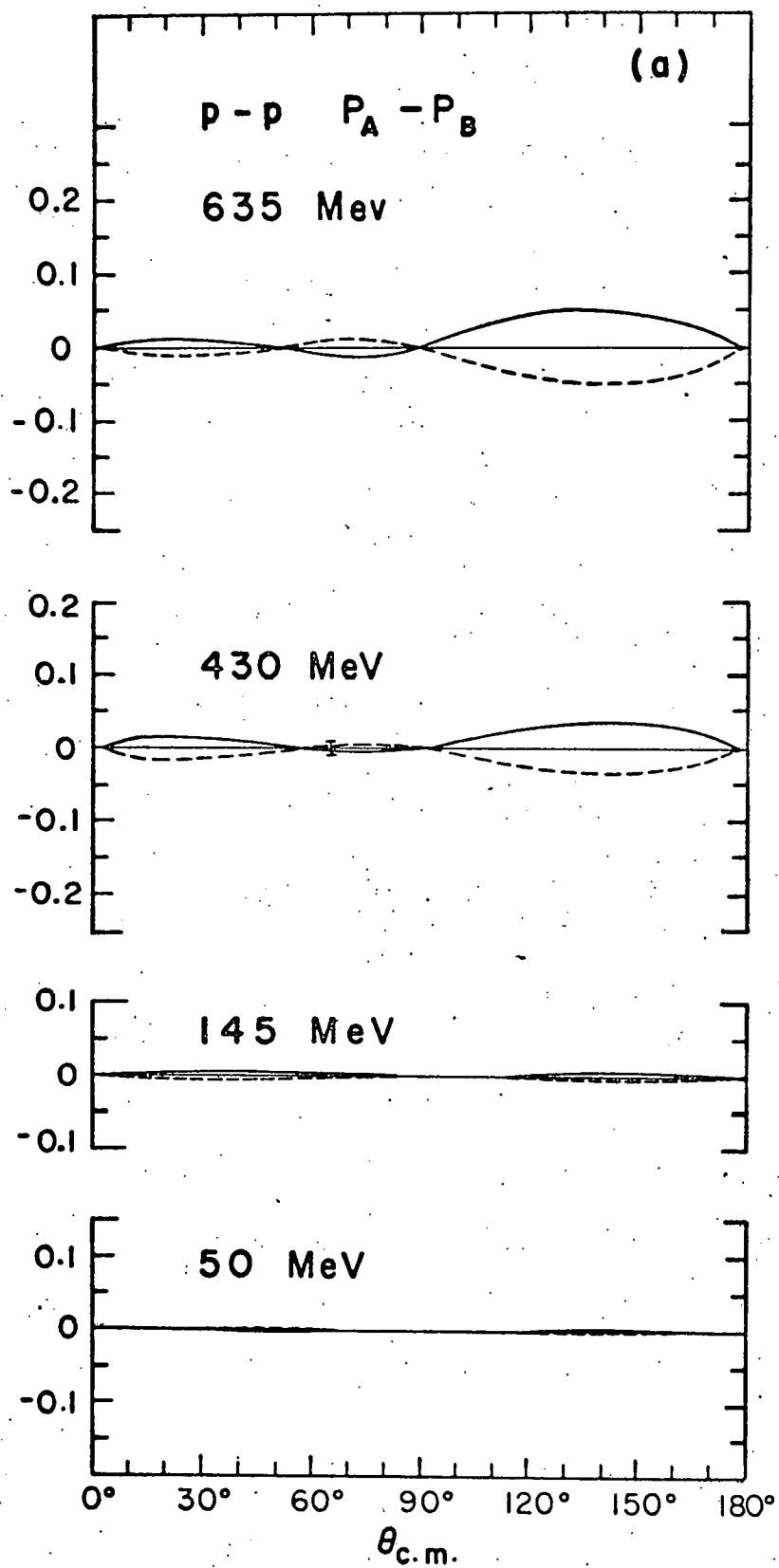


fig. 9b

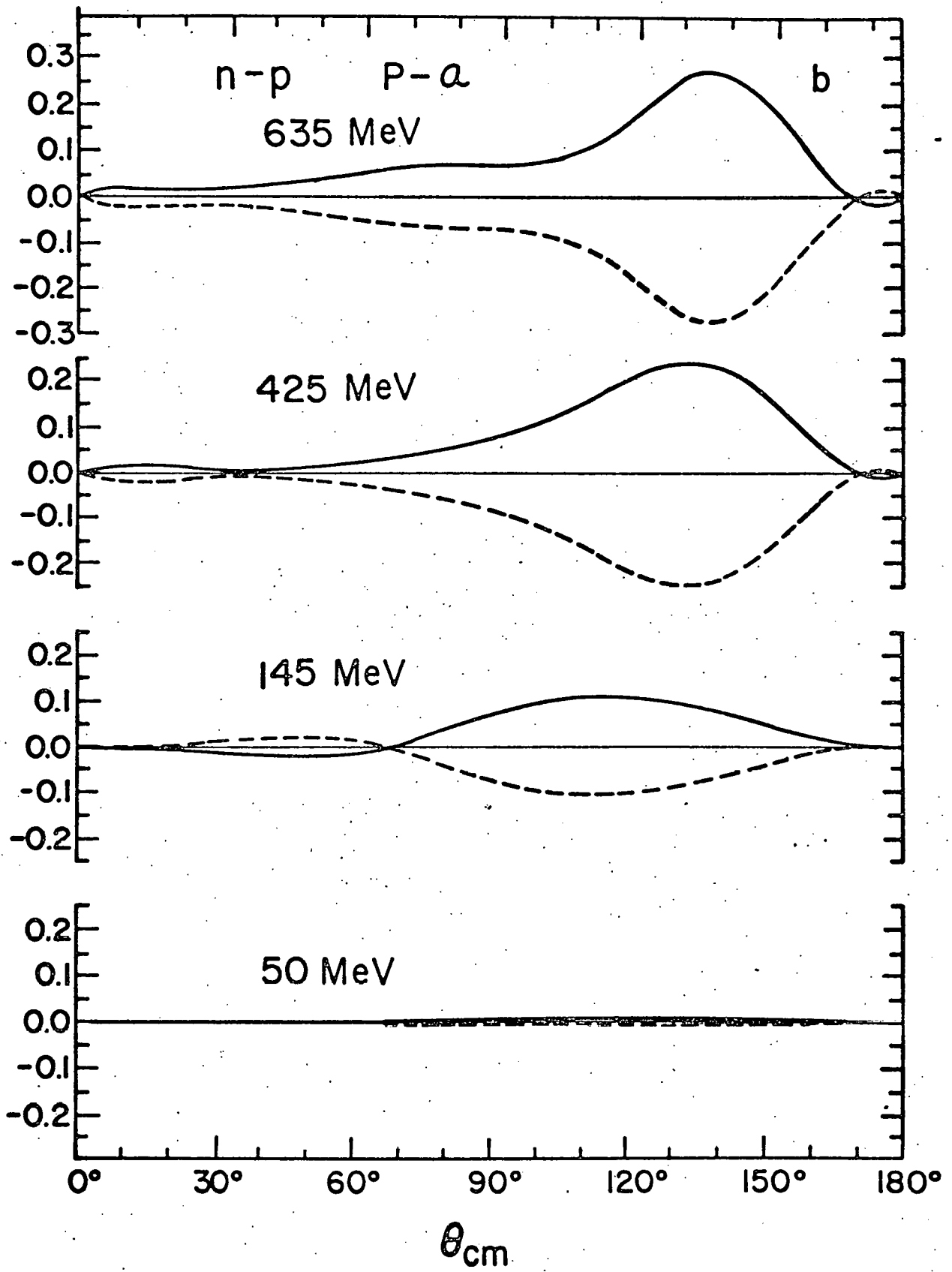


fig. 10a

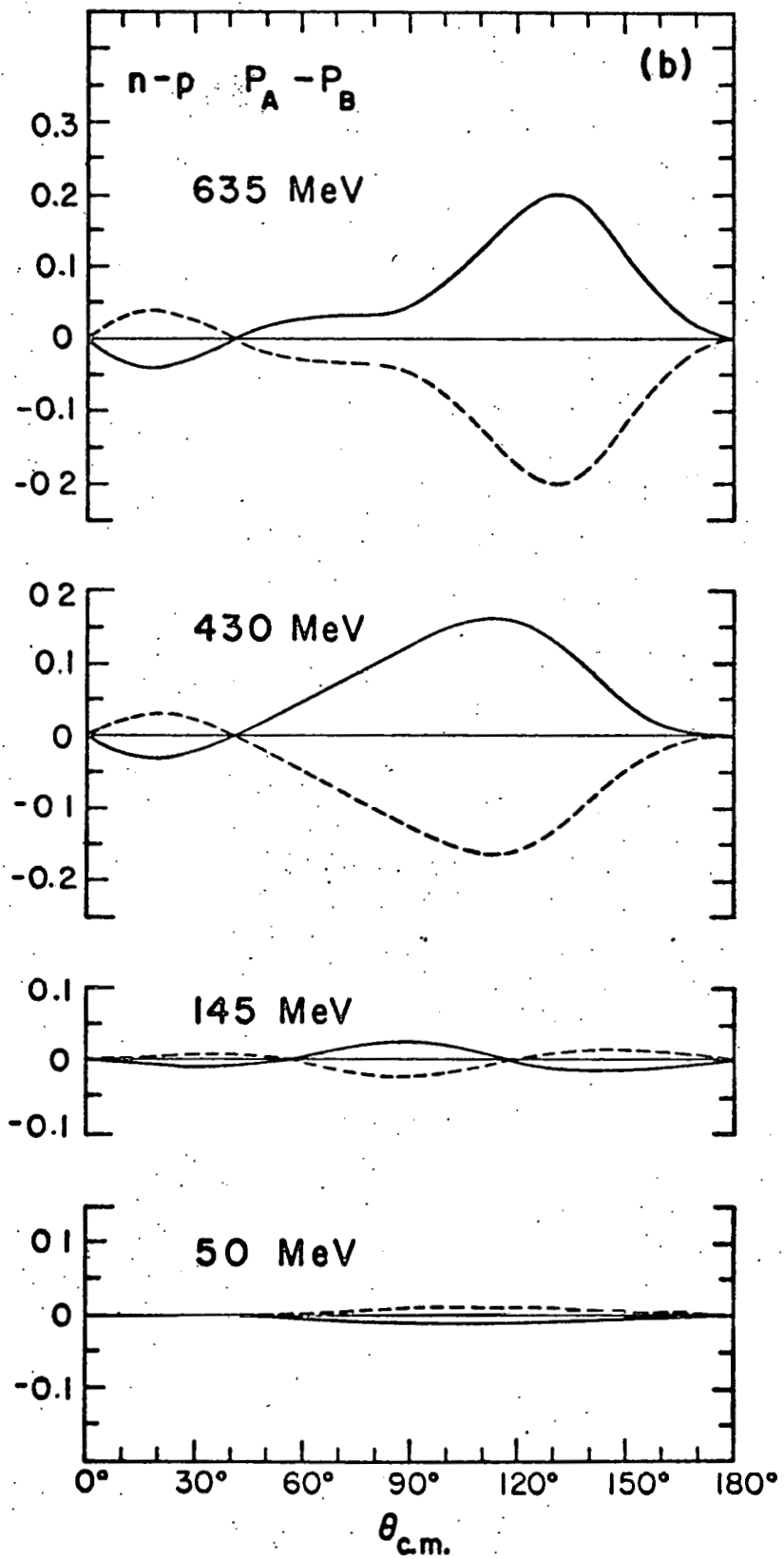


fig. 10b

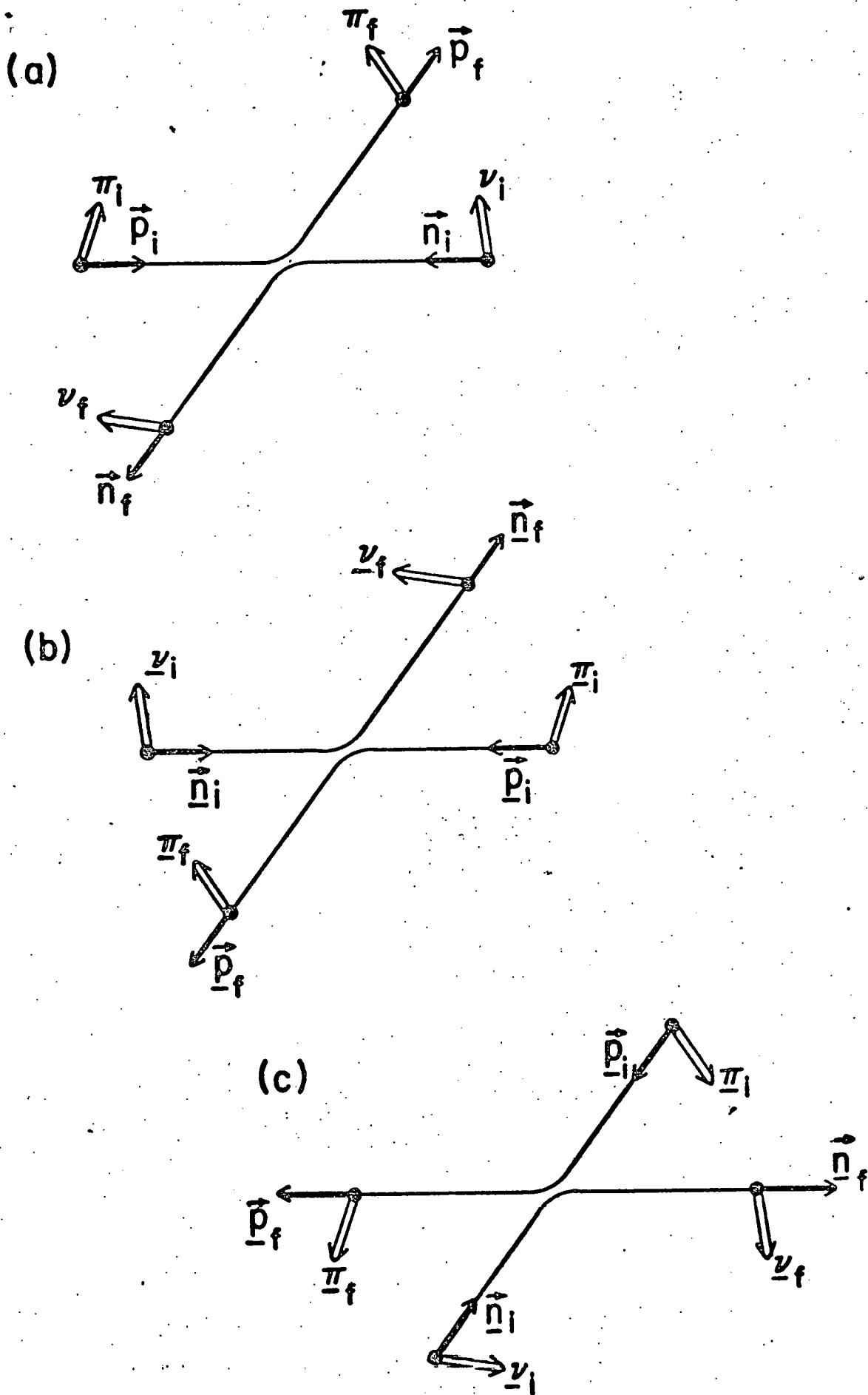
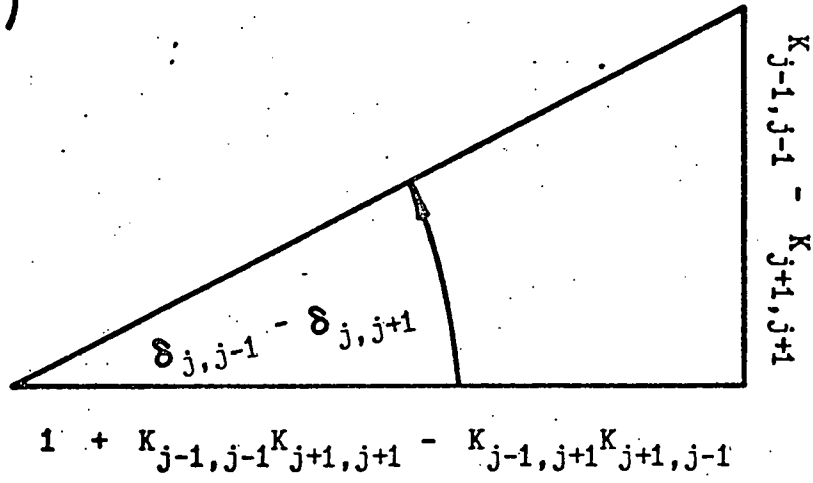


fig. 11

(a)



(b)

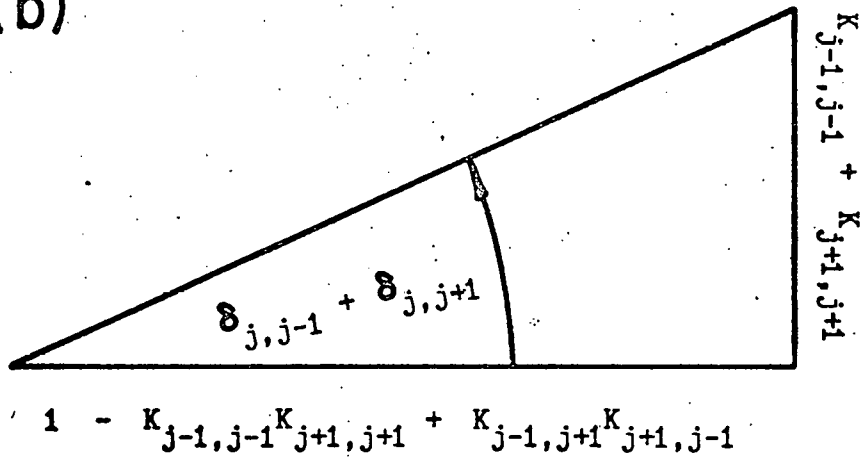


fig. 12

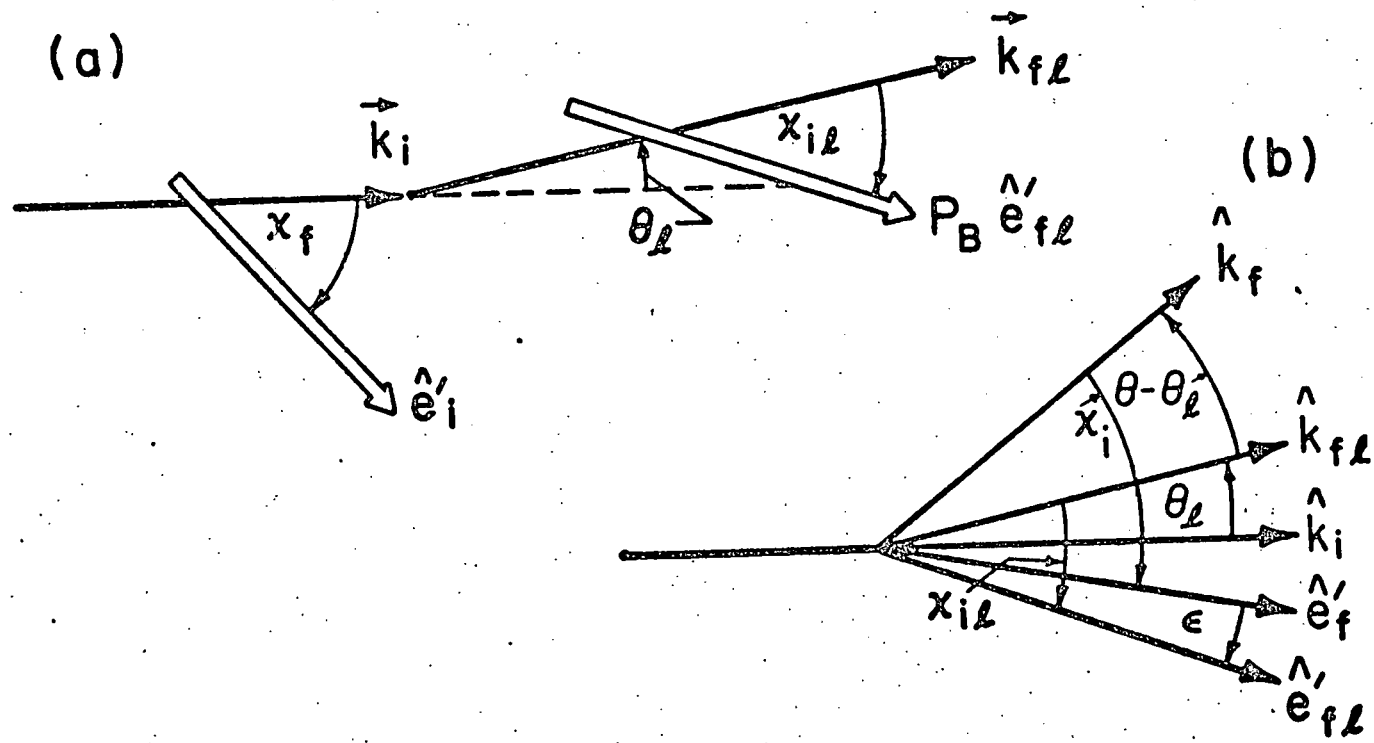


fig. 13

# Laboratory system

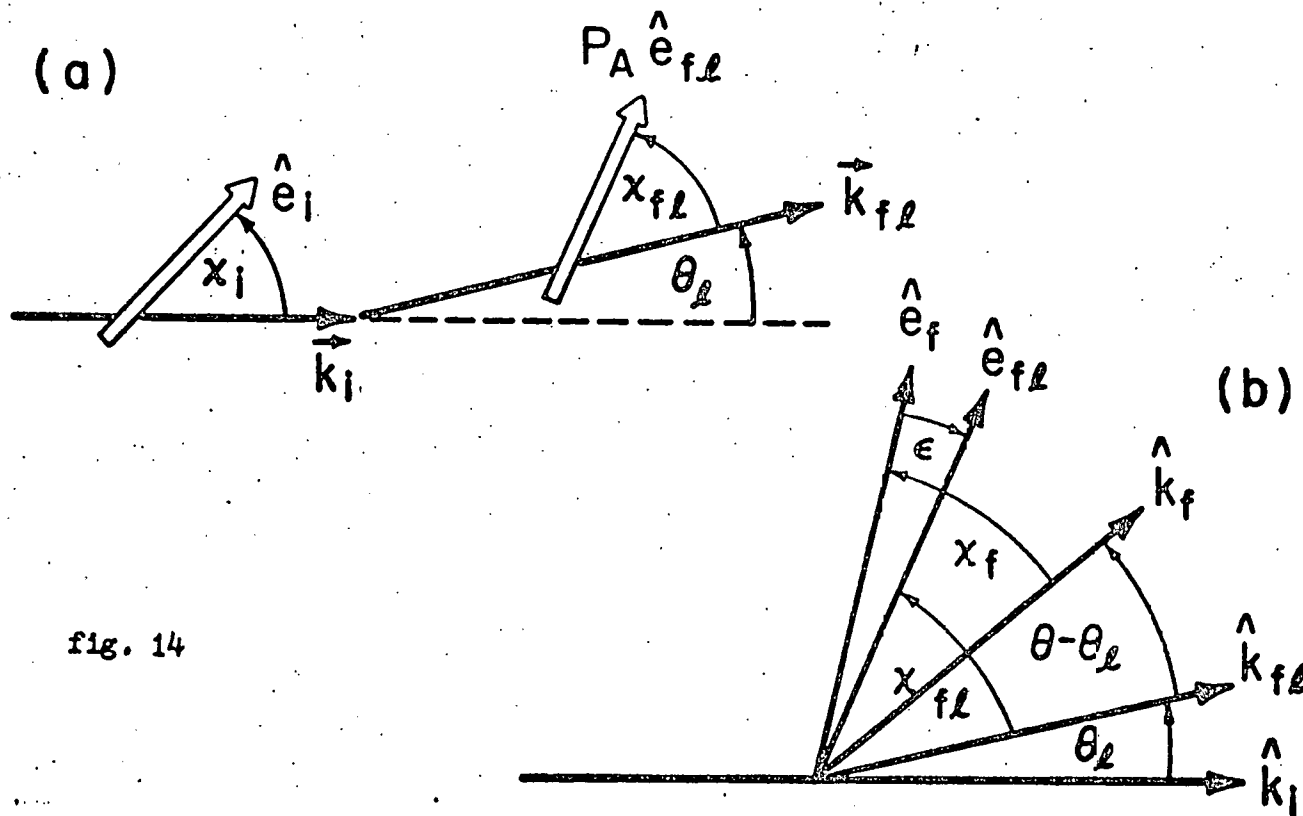


fig. 14